ESAIM: M2AN 49 (2015) 1193–1217
DOI: 10.1051/m2an/2015003

ESAIM: Mathematical Modelling and Numerical Analysis
www.esaim-m2an.org

ADAPTIVE CROUZEIX–RAVIART BOUNDARY ELEMENT METHOD *

Norbert Heuer[1] and Michael Karkulik[1]

Abstract. For the nonconforming Crouzeix–Raviart boundary elements from [N. Heuer and F.-J. Sayas, *Numer. Math.* **112** (2009) 381–401], we develop and analyze *a posteriori* error estimators based on the $h - h/2$ methodology. We discuss the optimal rate of convergence for uniform mesh refinement, and present a numerical experiment with singular data where our adaptive algorithm recovers the optimal rate while uniform mesh refinement is sub-optimal. We also discuss the case of reduced regularity by standard geometric singularities to conjecture that, in this situation, non-uniformly refined meshes are not superior to quasi-uniform meshes for Crouzeix–Raviart boundary elements.

Mathematics Subject Classification. 65N30, 65N38, 65N50, 65R20.

Received December 20, 2013. Revised November 7, 2014.
Published online June 30, 2015.

1. Introduction

This is the first paper on *a posteriori* error estimation and adaptivity for an *element-wise* nonconforming boundary element method, namely Crouzeix–Raviart boundary elements analyzed in [24]. Previously, in [13], we presented an error estimate for a boundary element method with nonconforming domain decomposition. There, critical for the analysis is that the nonconformity of the method stems from approximations that are discontinuous only across the interface of sub-domains, which are assumed to be fixed. In that case, the underlying energy norm of order 1/2 of discrete functions has to be localized only with respect to sub-domains. In this paper, where we consider approximations which are discontinuous across element edges, such sub-domain oriented arguments do not apply. Instead, we have to find localization arguments that are uniform under scalings with h, the diameter of elements, which is nontrivial in fractional order Sobolev spaces of order $\pm 1/2$.

The Crouzeix–Raviart boundary element method is of particular theoretical interest since it serves to set the mathematical foundation of (locally) nonconforming elements for the approximation of hypersingular integral equations. Our main theoretical result is the efficiency and reliability (based on a saturation assumption) of several *a posteriori* error estimators. Our second result is that, for problems with standard geometric singularities, Crouzeix–Raviart boundary elements with seemingly appropriate mesh refinement is as good as (and not better than) Crouzeix–Raviart boundary elements on quasi-uniform meshes. We further discuss this point below.

Keywords and phrases. Boundary element method, adaptive algorithm, nonconforming method, *a posteriori* error estimation.

* *Financial support by CONICYT through projects Anillo ACT1118 (ANANUM) and Fondecyt 1110324, 3140614 is gratefully acknowledged.*

[1] Facultad de Matemáticas, Pontificia Universidad Católica de Chile, Avenida Vicuña Mackenna, 4860 Santiago, Chile. mkarkulik@mat.puc.cl, nheuer@mat.puc.cl

The *a posteriori* error estimators in this work are based on the $h - h/2$-strategy. This strategy is well known from ordinary differential equations [22] and finite element methods [1,4]. Recently, it was applied to conforming boundary element methods [16,18] as well: if the discrete space X_ℓ is used to approximate the function ϕ in the energy norm $|||\cdot|||$, we use the uniformly refined space $\widehat{X}_\ell$ and the corresponding approximations Φ_ℓ and $\widehat{\Phi}_\ell$ to estimate the error *via* the heuristics

$$\eta_\ell := \left|\left|\left| \widehat{\Phi}_\ell - \Phi_\ell \right|\right|\right| \sim |||\phi - \Phi_\ell|||\,. \tag{1.1}$$

In a conforming setting, the proof of efficiency of η_ℓ (*i.e.*, it bounds the error from below) follows readily from orthogonality properties, while its reliability (*i.e.*, it is an upper bound of the error) is additionally based on a saturation assumption. In nonconforming methods, orthogonality is available only in a weaker form which contains additional terms, such that $h - h/2$-based estimators are more involved than in a conforming setting.

As mentioned before, additional difficulties arise in boundary element methods due to the fact that the underlying energy norm $|||\cdot|||$ is equivalent to a fractional order Sobolev norm. These norms typically cannot be split into local error indicators. We use ideas from [18] to localize *via* weighted integer order Sobolev norms.

Our model problem is a hypersingular integral equation on a plane open surface Γ. The energy norm of this problem defines a Sobolev space of order $1/2$, so that low-order conforming methods with quasi-uniform meshes have approximation order $\mathcal{O}(h^{s-1/2})$ (h being the mesh size) for $s \leq 2$, provided the exact solution has Sobolev regularity s. Typical solutions of hypersingular integral equations on open surfaces exhibit corner and corner-edge singularities, such that their regularity is restricted to orders $1 - \varepsilon$ for all $\varepsilon > 0$ [28]. In such a case, low-order conforming methods with quasi-uniform meshes have approximation orders equal to $\mathcal{O}(h^{1/2})$, *cf.* [6], while methods with appropriate shape-regular mesh refinement towards the singularities show an approximation order equal to $\mathcal{O}(h)$, *cf.* the discussion in [11], Section 7.3 (v). In [24] the authors have shown that exact solutions with Sobolev regularity 1 can be approximated by Crouzeix–Raviart boundary elements with order $\mathcal{O}(h^{1/2})$ on quasi-uniform meshes. For regularity $s \leq 2$, one could expect to recover the optimal rate $\mathcal{O}(h^{s-1/2})$ as in the conforming case. In addition, for appropriate shape-regular mesh refinement towards singularities or for adaptive methods, one could expect to recover the rate $\mathcal{O}(h)$ as in the conforming case.

Surprisingly, this appears to be false in the case of Crouzeix–Raviart boundary elements.

We conjecture that $\mathcal{O}(h^{1/2})$ (or $\mathcal{O}(N^{-1/4})$ with N being the number of unknowns) is the optimal rate for Crouzeix–Raviart boundary elements even when using non-uniformly refined meshes. We base our conjecture on two observations. Standard error estimation of nonconforming methods, based on the second Strang lemma, comprise a best-approximation term and a nonconformity term. The best-approximation term has indeed the optimal order of a conforming method but we observe that the standard upper bound of the nonconformity term is of the order $\mathcal{O}(N^{-1/4})$ and not better. This surprising result can be explained by the fact that the appearing Lagrangian multipliers on the edges of the elements (needed for the jump condition of the Crouzeix–Raviart basis functions) are approximated in a Sobolev space of order only $1/2$ less than the unknown function. Taking into account that the total relative measure of the edges increases with mesh refinement and that the Lagrangian multipliers are approximated only by constants, this explains the limited convergence order of the whole method. In Section 2.4, we discuss this behaviour in more detail.

The second observation stems from numerical experiments with Crouzeix–Raviart boundary elements using meshes which are optimal for *conforming* methods:

- We consider uniform meshes for the nonconforming approximation of a solution which is an element of the coarsest conforming space (*i.e.*, a conforming method would compute the exact solution). This numerical experiment is carried out in Section 2.4, and shows the conjectured convergence order $\mathcal{O}(h^{1/2})$.
- We consider algebraically graded meshes which are optimal for conforming approximations in the sense that they guarantee an approximation order $\mathcal{O}(N^{-1/2})$ for inherent singularities. These numerical experiments are carried out in Section 5.1, and confirm the conjectured order $\mathcal{O}(N^{-1/4})$.

Based on our conjecture, we conclude that, for Crouzeix–Raviart boundary elements, quasi-uniform meshes are optimal to approximate standard geometric singularities where the solution is almost in $H^1(\Gamma)$. There is no

need for adaptive mesh refinement. In this case, the only use of *a posteriori* error estimation is precisely error estimation, not adaptivity.

There are cases, however, where given data are singular so that solutions have singular behavior which is stronger than that due to geometric irregularities. In these cases an adaptive Crouzeix–Raviart boundary element method can be used to recover the optimal rate $\mathcal{O}(N^{-1/4})$ which cannot be achieved with quasi-uniform meshes in this situation. Our numerical experiments report on such a case where the exact solution is strictly less regular than $H^1(\Gamma)$.

As model problem, we use the Laplacian exterior to a polyhedral domain or an open polyhedral surface. The Neumann problem for such a problem can be written equivalently with the hypersingular integral operator $\mathcal{W}$,

$$\mathcal{W}\phi(\mathbf{x}) := -\frac{1}{4\pi}\partial_{\mathbf{n}(\mathbf{x})}\int_\Gamma \partial_{\mathbf{n}(\mathbf{y})}\left(\frac{1}{|\mathbf{x}-\mathbf{y}|}\right)\phi(\mathbf{y})\,d\Gamma(\mathbf{y}) = f(\mathbf{x}), \tag{1.2}$$

where Γ is the open or closed surface and f is a given function. The link to the Neumann problem for the exterior Laplacian is given by the special choice $f = (1/2 - K')v$, with v the Neumann datum and K' the adjoint of the double-layer operator. Although the operator $\mathcal{W}$ can act on discontinuous functions, the hypersingular integral equation (1.2) is not well-posed in such a case. However, continuity requirements can be relaxed by using the relation $\mathcal{W} = curl\mathcal{V}\mathbf{curl}$ with single layer operator $\mathcal{V}$ and certain surface differential operators *curl* and **curl**, see [20, 27]. This identity allows us to use the space V of Crouzeix–Raviart elements to approximate the exact solution ϕ of (1.2) in a nonconforming way. The associated energy norm will then be $|||\cdot||| = \|\mathbf{curl}\cdot\|_{H^{-1/2}(\Gamma)}$ (see Sect. 2.3).

The reliability and efficiency of $h - h/2$ error estimators for conforming methods follows readily from the Galerkin orthogonality

$$|||\phi - \Phi_\ell|||^2 = |||\phi - \Phi_\ell|||^2 + \left|\left|\left|\widehat{\Phi}_\ell - \Phi_\ell\right|\right|\right|^2, \tag{1.3}$$

where reliability additionally needs the saturation assumption

$$\left|\left|\left|\phi - \widehat{\Phi}_\ell\right|\right|\right| \le C_{\mathrm{sat}}\,|||\phi - \Phi_\ell|||\,, \qquad \text{with } 0 < C_{\mathrm{sat}} < 1 \text{ for all } \ell \in \mathbb{N}.$$

In a nonconforming setting, the orthogonality (1.3) does not hold true any longer. However, there is a substitute given by an estimate which involves additional terms of the form $\left|\left|\left|\Phi_\ell - \Phi_\ell^0\right|\right|\right|$, with Φ_ℓ^0 being a conforming approximation of ϕ, see Section 3.1.

A term of the form $\left|\left|\left|\Phi_\ell - \Phi_\ell^0\right|\right|\right|$ will be called *nonconformity error*. Although it is computable, it is evident that the computation of Φ_ℓ^0 has to be avoided. Hence, we will show that the nonconformity error can be bounded by inter-element jumps of Φ_ℓ, see Corollary 4.1. To that end, we will analyze the properties of quasi-interpolation operators in the space $H^{-1/2}(\Gamma)$ in Section 3.2.

In Section 4, we show that the *a posteriori* error estimator η_ℓ from (1.1) is reliable and efficient up to the nonconformity error, which can then be exchanged with the inter-element jumps of Φ_ℓ. As already mentioned, η_ℓ is not localized, and we will use ideas from [18] to introduce three additional error estimators for that purpose. Two of them are localized, see Section 4.2, and can be used in a standard adaptive algorithm, see Algorithm 1 below. We show in Section 4 that all error estimators are efficient and, under the saturation assumption, also reliable, up to inter-element jumps. Finally, Section 5 presents numerical results.

2. Crouzeix–Raviart boundary elements

2.1. Notation and model problem

We consider an open, plane, polygonal screen $\Gamma \subset \mathbb{R}^2$, embedded in $\mathbb{R}^3$, with normal $\mathbf{n}(\mathbf{y})$ at $\mathbf{y} \in \Gamma$ pointing upwards. Restricting ourselves to a plane screen simplifies the presentation. However, associated solutions exhibit

the strongest possible edge singularities that, at least for conforming methods, require nonuniform meshes in order to guarantee efficiency of approximation. On Γ, we use the standard spaces $L_2(\Gamma)$ and $H^1(\Gamma)$, and as usual, $H^1_0(\Gamma) \subset H^1(\Gamma)$ consists of functions that vanish on the boundary $\partial\Gamma$. The space $H^1_0(\Gamma)$ is equipped with the $H^1(\Gamma)$ (semi-)norm $|\cdot|_{H^1(\Gamma)} := \|\nabla_\Gamma \cdot\|_{L_2(\Gamma)}$ where ∇_Γ denotes the surface gradient. We define intermediate spaces by the K-method of interpolation (see, *e.g.*, [31]), that is,

$$H^s(\Gamma) = \big[L_2(\Gamma), H^1(\Gamma)\big]_s \quad \text{and} \quad \widetilde{H}^s(\Gamma) = \big[L_2(\Gamma), H^1_0(\Gamma)\big]_s \quad \text{for } 0 < s < 1.$$

Sobolev spaces with negative index are defined *via* duality with respect to the extended $L_2(\Gamma)$ inner product $\langle\cdot\,,\cdot\rangle$,

$$H^s(\Gamma) := \widetilde{H}^{-s}(\Gamma)' \quad \text{and} \quad \widetilde{H}^s(\Gamma) := H^{-s}(\Gamma)' \quad \text{for } -1 \le s < 0.$$

We also use the Sobolev-Slobodeckij semi-norm and norm defined by

$$|v|^2_{H^{1/2}_{\rm slo}(\omega)} := \int_\omega \int_\omega \frac{|v(\mathbf{x}) - v(\mathbf{y})|^2}{|\mathbf{x}-\mathbf{y}|^3}\, d\Gamma(\mathbf{x})\, d\Gamma(\mathbf{y}), \quad \|v\|^2_{H^{1/2}_{\rm slo}(\omega)} := \|v\|^2_{L_2(\omega)} + |v|^2_{H^{1/2}_{\rm slo}(\omega)}.$$

Space of vector valued functions will be denoted by bold-face letters, *i.e.* $\mathbf{L}_2(\Gamma)$ or $\mathbf{H}^{1/2}(\Gamma)$, meaning that every component is an element of the respective space. We will use tangential differential operators. For sufficiently smooth functions ϕ on Γ, we define the tangential curl operator **curl** by

$$\mathbf{curl}\phi := (\partial_y\phi, -\partial_x\phi, 0)\,.$$

Drawing upon the results from [9], it is shown in ([20], Lem. 2.2) that the operator **curl** can be extended to a continuous operator, mapping $\widetilde{H}^{1/2}(\Gamma)$ to

$$\widetilde{\mathbf{H}}^{-1/2}(\Gamma) := \big\{\psi \in \big(\widetilde{H}^{-1/2}(\Gamma)\big)^3 \mid \psi\cdot\mathbf{n} = 0\big\}.$$

Now our model problem is as follows. For a given $f \in H^{-1/2}(\Gamma)$, find $\phi \in \widetilde{H}^{1/2}(\Gamma)$ such that

$$\langle \mathcal{W}\phi\,, \psi\rangle = \langle f\,, \psi\rangle \quad \text{for all } \psi \in \widetilde{H}^{1/2}(\Gamma). \tag{2.1}$$

Here, $\mathcal{W}$ is the hypersingular integral operator from (1.2). It is well-known that this problem has a unique solution (*cf.* [28]). Recall the relation $\mathcal{W} = curl\mathcal{V}\mathbf{curl}$ with single layer operator $\mathcal{V}$,

$$\mathcal{V}u(\mathbf{x}) := \frac{1}{4\pi}\int_\Gamma \frac{1}{|\mathbf{x}-\mathbf{y}|} u(\mathbf{y})\, d\Gamma(\mathbf{y}).$$

Performing integration by parts one finds that an equivalent formulation of (2.1) is given by

$$\langle \mathcal{V}\mathbf{curl}\phi\,, \mathbf{curl}\psi\rangle = \langle f\,, \psi\rangle \quad \text{for all } \psi \in \widetilde{H}^{1/2}(\Gamma), \tag{2.2}$$

see ([27] and [20], Lem. 2.3). Note that $\mathcal{V}$ in (2.2) is considered to transfer *vectorial* densities into *vectorial* potentials, *i.e.*, $\mathcal{V}$ acts component-wise.

2.2. Meshes and local mesh-refinement

A triangulation $\mathcal{T}$ of Γ consists of compact 2-dimensional simplices (*i.e.*, triangles) T such that $\bigcup_{T\in\mathcal{T}} T = \overline{\Gamma}$. We do not allow hanging nodes. The volume area $|T|$ of every element defines the local mesh-width $h_\mathcal{T} \in L_\infty(\Gamma)$ by $h_\mathcal{T}|_T := h_\mathcal{T}(T) := |T|^{1/2}$. We define $\mathcal{E}_\mathcal{T}$ to be the set of all edges e of the triangulation $\mathcal{T}$, and $\mathcal{N}_\mathcal{T}$ as the set of all nodes z of the triangulation which are not on the boundary $\partial\Gamma$. We will need different kinds of patches.

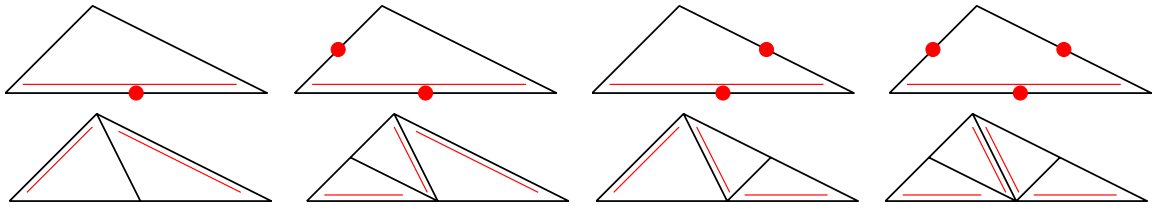

FIGURE 1. For each triangle $T \in \mathcal{T}_\ell$, there is one fixed *reference edge*, indicated by the double line (*left, top*). Refinement of T is done by bisecting the reference edge, where its midpoint becomes a new node. The reference edges of the son triangles $T' \in \mathcal{T}_{\ell+1}$ are opposite to this newest vertex (*left, bottom*). To avoid hanging nodes, one proceeds as follows: we assume that certain edges of T, but at least the reference edge, are marked for refinement (*top*). Using iterated newest vertex bisection, the element is then split into 2, 3, or 4 son triangles (*bottom*). If all elements are refined by three bisections (*right, bottom*), we obtain the so-called uniform bisec(3)-refinement which is denoted by $\widehat{\mathcal{T}}_\ell$.

For a node $z \in \mathcal{N}_\mathcal{T}$, we denote by ω_z the node patch as the set of all elements $T \in \mathcal{T}$ sharing z. Likewise, we define an edge patch ω_e. For an element $T \in \mathcal{T}$, the patch ω_T is the set of all elements sharing a node with T.

Starting from an initial triangulation $\mathcal{T}_0$ of Γ, we will generate a sequence of meshes $\mathcal{T}_\ell$ for $\ell \in \mathbb{N}$ *via* so-called *newest vertex bisection* (NVB). For a brief overview, we refer to Figure 1, and for a precise definition, we refer the reader to [32]. In order to terminate, a recursive definition of NVB requires the coarse mesh $\mathcal{T}_0$ to be equipped with a special reference edge labeling (an edge is reference edge of both its adjacent elements or of none). In [7], such a labeling is also needed to derive a complexity bound which is used in proving optimal convergence rates of adaptive algorithms. The recent work [25] presents an iterative definition of the NVB algorithm which does not need a special labeling to terminate, and shows also that the complexity bound stays valid. Hence, we do not need to specify any labeling of reference edges. We denote by $\overline{T}$ a fixed reference element, and by $\overline{u}$ the pull-back of a function u defined on T, *i.e.*, if $F_T : \overline{T} \to T$ is the affine element map, $\overline{u} := u \circ F_T$. An important property of the NVB refinement strategy is that one can not only map elements T to fixed reference domains, but also patches. This means that there is a finite set of fixed reference patches and affine maps such that any node-, element-, or edge patch is the affine image of such a reference patch. In particular, there are only finitely many constants involved in scaling argument on patches, and hence, one may use patches in scaling arguments. For a mesh $\mathcal{T}$, we denote by $\widehat{\mathcal{T}}$ the uniformly refined mesh, *i.e.*, all edges in $\mathcal{T}$ are bisected.

For a triangle $T \in \mathcal{T}$, we denote by $\mathbf{n}_T$ the normal vector on ∂T pointing outwards of T. For an inner edge $e \in \mathcal{E}_\mathcal{T}$, *i.e.*, $e \subset \Gamma$, we denote by T_e^+ and T_e^- the two elements of $\mathcal{T}$ sharing e, and we define $\mathbf{n}^+ := \mathbf{n}_{T_e^+}$ and $\mathbf{n}^- := \mathbf{n}_{T_e^-}$. For smooth enough functions $\phi : \Gamma \to \mathbb{R}$ and $\mathbf{v} : \Gamma \to \mathbb{R}^2$ we define the jumps $[\![\cdot]\!]$ and averages $\{\cdot\}$ of the traces ϕ^+, ϕ^-, $\mathbf{v}^+$, and $\mathbf{v}^-$ by

$$\{\phi\}|_e := \tfrac{1}{2}(\phi^+ + \phi^-), \quad \{\mathbf{v}\}|_e := \tfrac{1}{2}(\mathbf{v}^+ + \mathbf{v}^-),$$
$$[\![\phi]\!]|_e := \phi^+\mathbf{n}^+ + \phi^-\mathbf{n}^-, \; [\![\mathbf{v}]\!]|_e := \mathbf{v}^+\mathbf{n}^+ + \mathbf{v}^-\mathbf{n}^-.$$

We will frequently use the arc length derivative of the jump of functions on the edges $\mathcal{E}_\mathcal{T}$. This will be denoted by $[\![\cdot]\!]'$. If we equip a mesh with an index, *e.g.*, $\mathcal{T}_\ell$, then we will use the index $(\cdot)_\ell$ instead of $(\cdot)_{\mathcal{T}_\ell}$, *i.e.*, we write, *e.g.*, h_ℓ instead of $h_{\mathcal{T}_\ell}$, and the same abbreviation will be used for sets of edges or nodes, *e.g.*, $\mathcal{E}_\ell$ or $\mathcal{N}_\ell$.

2.3. Crouzeix–Raviart boundary elements

For a given mesh $\mathcal{T}$, $\mathcal{P}^1(\mathcal{T})$ is the space of piecewise linear functions. By $V^0 = V^0_\mathcal{T}$, we denote the space of lowest-order continuous boundary elements, *i.e.*,

$$V^0 := \mathcal{P}^1(\mathcal{T}) \cap H^1_0(\Gamma),$$

and $V = V_{\mathcal{T}}$ is the space of Crouzeix–Raviart boundary elements, *i.e.*,

$$V := \left\{ \Phi \in \mathcal{P}^1(\mathcal{T}) \;\middle|\; \begin{array}{r} \Phi \text{ is continuous in } \mathbf{m}_e \; \forall e \in \mathcal{E}_{\mathcal{T}} \text{ with } e \nsubseteq \partial\Gamma, \\ \Phi(\mathbf{m}_e) = 0 \; \forall e \in \mathcal{E}_{\mathcal{T}} \text{ with } e \subset \Gamma \end{array} \right\},$$

where $\mathbf{m}_e$ is the midpoint of $e \in \mathcal{E}_{\mathcal{T}}$. For $\mathbf{curl}_{\mathcal{T}} : \mathcal{P}^1(\mathcal{T}) \to \mathbf{L}_2(\Gamma)$ being the $\mathcal{T}$-piecewise tangential curl operator, a norm in V is given by

$$|||\cdot|||_{\mathcal{T}} := \|\mathbf{curl}_{\mathcal{T}} \cdot\|_{\widetilde{\mathbf{H}}^{-1/2}(\Gamma)}.$$

In the following we consider the bilinear form

$$a_{\mathcal{T}}(\Phi, \Psi) := \langle \mathcal{V}\mathbf{curl}_{\mathcal{T}}\Phi \,, \mathbf{curl}_{\mathcal{T}}\Psi \rangle .$$

By the properties of the single-layer operator $\mathcal{V}$ (*cf.* [26]), $a_{\mathcal{T}}$ is symmetric and there is a constant $C_{\rm norm} > 1$, independent of $\mathcal{T}$ and $\Phi \in V$, such that

$$C_{\rm norm}^{-2} \, |||\Phi|||_{\mathcal{T}}^2 \le a_{\mathcal{T}}(\Phi, \Phi) \le C_{\rm norm}^2 \, |||\Phi|||_{\mathcal{T}}^2 .$$

This makes $a_{\mathcal{T}}$ an inner product in V, which is therefore a Hilbert space. Assuming additional regularity $f \in H^{-1/2+\varepsilon}(\Gamma)$ with $\varepsilon > 0$, then

$$\langle f \,, \Psi \rangle \le \|f\|_{H^{-1/2+\varepsilon}(\Gamma)} \, \|\Psi\|_{H^{1/2-\varepsilon}(\Gamma)} \le C_{\mathcal{T}} \, |||\Psi|||_{\mathcal{T}} \qquad \text{for all } \Psi \in V. \tag{2.3}$$

Here we used the equivalence of norms in the finite-dimensional space V, such that the number $C_{\mathcal{T}} > 0$ depends on $\mathcal{T}$. By the Lax–Milgram lemma there exists a unique Galerkin solution $\Phi \in V$ of

$$\langle \mathcal{V}\mathbf{curl}_{\mathcal{T}}\Phi \,, \mathbf{curl}_{\mathcal{T}}\Psi \rangle = \langle f \,, \Psi \rangle \qquad \text{for all } \Psi \in V. \tag{2.4}$$

The unique solvability of (2.4) was already addressed in [24] and studied *via* an equivalent saddle-point problem. We emphasize that the constant $C_{\mathcal{T}}$ in (2.3) depends on V, but is not used in our analysis. In the statements and arguments below, our notations will mostly omit the explicit dependence on $\mathcal{T}$ by writing, *e.g.*, $|||\cdot|||$, assuming that this is the norm related to the finest mesh which occurs in the norms' argument.

2.4. Uniform refinement: consistency error and optimal convergence

We briefly discuss existing results for the Crouzeix–Raviart BEM of Section 2.3 based on a sequence of uniformly refined meshes $(\mathcal{T}_\ell)_{\ell \in \mathbb{N}_0}$. According to Theorem 2 of [24], it holds that

$$|||\phi - \Phi_\ell||| \lesssim h_\ell^{1/2} \, \|\phi\|_{H^1(\Gamma)} , \tag{2.5}$$

if $f \in L_2(\Gamma)$ and $(\mathcal{T}_\ell)_{\ell \in \mathbb{N}_0}$ is a uniform sequence of meshes with mesh width h_ℓ. The proof of (2.5) uses, as is customary in the analysis of nonconforming methods, the Lemma of Berger, Scott, and Strang (*cf.* [5]), which states that the error is bounded by the sum of best-approximation error and consistency error,

$$|||\phi - \Phi_\ell||| \le \inf_{\Phi_\ell^0 \in V_\ell^0} |||\phi - \Phi_\ell^0||| + \sup_{\Psi_\ell \in V_\ell} \frac{a_{\mathcal{T}}(\phi - \Phi_\ell, \Psi_\ell)}{|||\Psi_\ell|||}.$$

The best-approximation error behaves at least as good as the one of a conforming method, such that it is essential to bound the consistency error. In Proposition 5 of [24], it is shown that

$$\sup_{\Psi_\ell \in V_\ell} \frac{a_{\mathcal{T}}(\phi - \Phi_\ell, \Psi_\ell)}{|||\Psi_\ell|||} \lesssim \inf_{\mu_\ell \in \mathcal{P}^0(\mathcal{E}_\ell)} \left[\sum_{e \in \mathcal{E}_\ell} \|\mathbf{t}_e \cdot \mathcal{V}\mathbf{curl}\phi - \mu_\ell\|_{L_2(e)}^2 \right]^{1/2}. \tag{2.6}$$

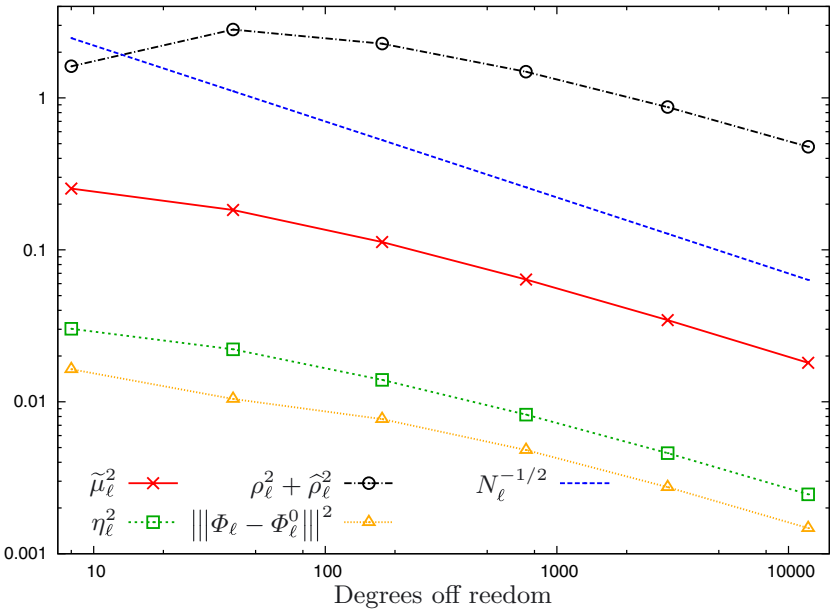

FIGURE 2. Convergence rates for uniform mesh refinement and solution which is already in the coarsest conforming space. We plot squared quantities so that $\mathcal{O}(N_\ell^{-1/2})$ corresponds to a rate of $\mathcal{O}(h_\ell^{1/2})$ for the original quantities. The quantities $\widetilde{\mu}_\ell$ and η_ℓ are error estimators which will be defined in Section 4. The quantities ρ_ℓ and $\widehat{\rho}_\ell$ are bounds for $|||\Phi_\ell - \Phi_\ell^0|||$ which measure the deviation of the nonconforming solution Φ_ℓ from its conforming counterpart Φ_ℓ^0 (*cf.* Cor. 4.1 below). We see that $|||\Phi_\ell - \Phi_\ell^0||| \simeq \mathcal{O}(N_\ell^{-1/4})$. Due to (2.7), this order of convergence also holds for the energy error $|||\phi - \Phi_\ell|||$.

The space $\mathcal{P}^0(\mathcal{E}_\ell)$ in (2.6) arises from integrating by parts element-wise the term $a_\mathcal{T}(\phi - \Phi_\ell, \Psi_\ell)$ and then using the fact that as Ψ_ℓ is a Crouzeix–Raviart function, its jump has vanishing integral mean on every edge $e \in \mathcal{E}_\ell$. Hence, $\mathcal{E}_\ell$-piecewise constants can be inserted and the infimum can be taken. In Lemma 6 of [24], it is shown that the right-hand side in (2.6) converges like $\mathcal{O}(h_\ell^{1/2})$ given that $\phi \in H^1(\Gamma)$. However, this bound for the convergence rate of the right-hand side is optimal. Indeed, even for $v \in \mathcal{P}^1(\Gamma) \setminus \mathcal{P}^0(\Gamma)$ it only holds that

$$\inf_{\mu_\ell \in \mathcal{P}^0(\mathcal{E}_\ell)} \left[\sum_{e \in \mathcal{E}_\ell} \|v - \mu_\ell\|_{L_2(e)}^2 \right]^{1/2} \simeq \mathcal{O}\left(h_\ell^{1/2}\right),$$

which can be seen by a direct calculation. The total error is also bounded from below by the consistency error due to the continuity of the bilinear form, *i.e.*,

$$\sup_{\Psi_\ell \in V_\ell} \frac{a_\mathcal{T}(\phi - \Phi_\ell, \Psi_\ell)}{|||\Psi_\ell|||} \lesssim |||\phi - \Phi_\ell|||.$$

Thus, we are led to conjecture that the optimal order of convergence is $\mathcal{O}(h^{1/2})$. To prove our conjecture it is enough to show that the estimate in (2.6) is indeed an equivalence. There is no apparent loss of approximation order in (2.6), but its equivalence is an open problem. A simple numerical example supports our conjecture (and more experiments are performed below). We choose $\Gamma = [0,1]^2$ and divide it along the diagonals and the midpoints of its sides, such that we obtain a mesh $\mathcal{T}_0$ of 8 triangles. We choose the exact solution $\phi \in V_0^0$ that vanishes on $\partial\Gamma$ and has the value 1 in the center of Γ. In Figure 2, we visualize the outcome of the corresponding

Crouzeix–Raviart BEM based on a uniform mesh refinement. We have not yet defined the shown quantities, but what is important here is that $\Phi_\ell \in V_\ell$ denotes the Crouzeix–Raviart solution on the mesh $\mathcal{T}_\ell$, whereas $\Phi_\ell^0 \in V_\ell^0$ denotes the conforming solution. According to the definition of ϕ, we have $\Phi_\ell^0 = \phi$, and hence, according to (2.5),

$$|||\phi - \Phi_\ell||| = \big|||\Phi_\ell - \Phi_\ell^0|||\big| = \mathcal{O}\left(h_\ell^{1/2}\right). \tag{2.7}$$

One would expect an increased order of $\mathcal{O}(h_\ell^{1-\varepsilon})$ for every $\varepsilon > 0$, as $\phi \in \widetilde{H}^{1/2}(\Gamma) \cap H^{3/2-\varepsilon}(\Gamma)$. However, as Figure 2 reveals, this increased rate is not achieved – we still observe $\mathcal{O}(h_\ell^{1/2})$, which therefore seems to be the optimal rate that can be obtained.

3. Preliminaries

3.1. Conforming approximations and partial orthogonality

For the development and analysis of the adaptive Crouzeix–Raviart boundary elements, it will be convenient to use a decomposition of the space $V_\mathcal{T}$ into conforming and nonconforming components. Such a decomposition is given by the identity

$$V_\mathcal{T} = V_\mathcal{T}^0 \oplus V_\mathcal{T}^\perp,$$

where $V_\mathcal{T}^\perp$ is the orthogonal complement of $V_\mathcal{T}^0$ with respect to the inner product $a_\mathcal{T}(\cdot,\cdot)$. For a function $\Phi \in V_\mathcal{T}$, we write $\Phi = \Phi^0 + \Phi^\perp$ with $\Phi^0 \in V_\mathcal{T}^0$ and $\Phi^\perp \in V_\mathcal{T}^\perp$. We emphasize that there is a partial orthogonality, *i.e.*, if $\mathcal{T}_\star$ is a refinement of $\mathcal{T}$, then

$$a_\star(\phi - \Phi_\star, \Psi) = 0 \quad \text{for all } \Psi \in V_\mathcal{T}^0,$$

where ϕ is the exact solution and $\Phi_\star \in V_{\mathcal{T}_\star}$ is its nonconforming Galerkin approximation. In contrast to conforming methods, this orthogonality property cannot be extended to all $\Psi \in V_\mathcal{T}$. However, it can be extended to a partial orthogonality as follows (*cf.* [8], Cor. 4.3).

Lemma 3.1. *Let $\mathcal{T}_\star$ be a refinement of $\mathcal{T}$ and $\Phi_\star \in V_{\mathcal{T}_\star}$ the Galerkin solution (2.4) on $\mathcal{T}_\star$. Then, for all $\varepsilon > 0$, and all $\Phi \in V_\mathcal{T}$, we have*

$$\begin{aligned} a_\star(\phi - \Phi_\star, \phi - \Phi_\star) &\le (1+\varepsilon) a(\phi - \Phi, \phi - \Phi) \\ &\quad - \frac{C_{\mathrm{norm}}^{-2}}{2} |||\Phi - \Phi_\star|||_\star^2 + \left(C_{\mathrm{norm}}^2 \left(1 + \frac{1}{\varepsilon}\right) + C_{\mathrm{norm}}^{-2}\right) \big|||(\Phi - \Phi^0) - (\Phi_\star - \Phi_\star^0)\big|||_\star^2 \end{aligned}$$

Proof. As $\phi - \Phi_\star$ is orthogonal to $V_\mathcal{T}^0$ and $V^0(\mathcal{T}_\star)$, we have

$$\begin{aligned} a_\star(\phi - \Phi_\star, \phi - \Phi_\star) &= a_\star\left(\phi - \Phi_\star - \Phi^0 + \Phi_\star^0, \phi - \Phi_\star - \Phi^0 + \Phi_\star^0\right) - a_\star\left(\Phi_\star^0 - \Phi^0, \Phi_\star^0 - \Phi^0\right) \\ &= a_\star\left(\phi - \Phi + \Phi^\perp - \Phi_\star^\perp, \phi - \Phi + \Phi^\perp - \Phi_\star^\perp\right) - a_\star\left(\Phi_\star^0 - \Phi^0, \Phi_\star^0 - \Phi^0\right) \\ &= a_\star(\phi - \Phi, \phi - \Phi) + 2a_\star\left(\Phi^\perp - \Phi_\star^\perp, \phi - \Phi\right) \\ &\quad + a_\star\left(\Phi^\perp - \Phi_\star^\perp, \Phi^\perp - \Phi_\star^\perp\right) - a_\star\left(\Phi_\star^0 - \Phi^0, \Phi_\star^0 - \Phi^0\right), \end{aligned}$$

where we used the identity $\Phi_\star + \Phi^0 - \Phi_\star^0 = \Phi - \Phi^\perp + \Phi_\star^\perp$ in the second step. Using the stability, ellipticity, and Young's inequality $ab \le a^2/(4\varepsilon) + \varepsilon b^2$, we obtain

$$\begin{aligned} 2a_\star\left(\phi - \Phi, \Phi^\perp - \Phi_\star^\perp\right) &\le 2a(\phi - \Phi, \phi - \Phi)^{1/2} a_\star\left(\Phi^\perp - \Phi_\star^\perp, \Phi^\perp - \Phi_\star^\perp\right)^{1/2} \\ &\le \varepsilon a(\phi - \Phi, \phi - \Phi) + \varepsilon^{-1} C_{\mathrm{norm}}^2 \big|||\Phi^\perp - \Phi_\star^\perp|||_\star^2, \end{aligned}$$

as well as

$$\frac{C_{\mathrm{norm}}^{-2}}{2}\,|||\Phi_\star-\Phi|||_\star^2-C_{\mathrm{norm}}^{-2}\,|||\Phi_\star^\perp-\Phi^\perp|||_\star^2\le C_{\mathrm{norm}}^{-2}\,|||\Phi_\star^0-\Phi^0|||_\star^2\le a_\star\left(\Phi_\star^0-\Phi^0,\Phi_\star^0-\Phi^0\right).$$

Finally, the estimate

$$a_\star\left(\Phi^\perp-\Phi_\star^\perp,\Phi^\perp-\Phi_\star^\perp\right)\le C_{\mathrm{norm}}^2\,|||\Phi^\perp-\Phi_\star^\perp|||_\star^2$$

concludes the proof. □

3.2. Quasi-interpolation operators in $\widetilde{\mathbf{H}}^{-1/2}(\Gamma)$

Lemma 3.1 will be the basis for the analysis of the *a posteriori* error estimators in Section 4, such that terms of the form $|||\Phi-\Phi^0|||$ will emerge. Those terms are (in principle) computable. However, they involve conforming approximations Φ^0, which we do not want to compute, and hence we need to find a substitute involving only Φ. This will be done in Corollary 4.1, where we will estimate the nonconformity of a function Φ by its jumps over edges. The proof of this corollary will be based on results of the present section, the aim of which is to provide an interpolation operator to approximate the conforming part Φ^0 of a given function Φ. We will use the well-known interpolation operator $I_{\mathcal{T}}$ by Clément [12,29], and provide approximation results in the space $\widetilde{\mathbf{H}}^{-1/2}(\Gamma)$. For a function $v\in L_2(\Gamma)$, this operator is defined as

$$I_{\mathcal{T}}v:=\sum_{z\in\mathcal{N}_{\mathcal{T}}}\psi(z)\varphi_z,\tag{3.1}$$

where φ_z is the nodal basis function of $V_{\mathcal{T}}^0$ associated with the node $z\in\mathcal{N}_{\mathcal{T}}$. The function $\psi\in V_{\mathcal{T}}^0|_{\omega_z}$ is such that

$$\int_{\omega_z}(v-\psi)\varphi=0\quad\text{ for all }\varphi\in V_{\mathcal{T}}^0|_{\omega_z}$$

see also ([8], Lem. 6.6). In addition, we denote by $\Pi_{\mathcal{T}}$ the $L_2(\Gamma)$ orthogonal projection onto the space of piecewise constants $[\mathcal{P}^0(\mathcal{T})]^2$. The well-known properties of the operator $I_{\mathcal{T}}$ are collected in the following lemma. We again refer to ([8], Lem. 6.6) for a proof.

Lemma 3.2. *Let $\mathcal{T}$ be a refinement of $\mathcal{T}_0$. Then, there exists a constant C_{I} which depends only on $\mathcal{T}_0$ such that*

$$\|I_{\mathcal{T}}\varphi\|_{L_2(\Gamma)}\le C_{\mathrm{I}}\,\|\varphi\|_{L_2(\Gamma)}\quad\text{ and }\quad\|I_{\mathcal{T}}\varphi\|_{H^1(\Gamma)}\le C_{\mathrm{I}}\,\|\varphi\|_{H^1(\Gamma)},\tag{3.2}$$

and such that for all $T\in\mathcal{T}$, for all $\varphi\in H_0^1(\Gamma)$, and for all $\Phi\in V_{\mathcal{T}}$, it holds that

$$\|\varphi-I_{\mathcal{T}}\varphi\|_{L_2(T)}\le C_{\mathrm{I}}\,\|h_{\mathcal{T}}\nabla\varphi\|_{\mathbf{L}_2(\omega_T)},\tag{3.3a}$$

$$\|\Phi-I_{\mathcal{T}}\Phi\|_{L_2(T)}\le C_{\mathrm{I}}\left\|h_{\mathcal{T}}^{1/2}\,[\![\Phi]\!]\right\|_{L_2(\mathcal{E}_{\omega_T})},\tag{3.3b}$$

$$\|\nabla_{\mathcal{T}}(\Phi-I_{\mathcal{T}}\Phi)\|_{\mathbf{L}_2(T)}\le C_{\mathrm{I}}\left\|h_{\mathcal{T}}^{-1/2}\,[\![\Phi]\!]\right\|_{L_2(\mathcal{E}_{\omega_T})},\tag{3.3c}$$

where $\nabla_{\mathcal{T}}$ is the $\mathcal{T}$-piecewise gradient.

For our purposes, we need to analyze the properties of $I_{\mathcal{T}}$ in the space $\widetilde{\mathbf{H}}^{-1/2}(\Gamma)$. To do so, we will use integration by parts piecewise. The resulting integrals over the skeleton $\mathcal{E}_{\mathcal{T}}$ will be bounded with the aid of the following auxiliary result.

Lemma 3.3. *Let $\mathcal{T}$ be a refinement of $\mathcal{T}_0$ with the set of edges $\mathcal{E}_\mathcal{T}$. Then, there is a constant $C_{\rm edge}$ which depends only on $\mathcal{T}_0$ such that for any choice of functions $\Phi \in V_\mathcal{T}$ and $\mathbf{V} \in \big[V_\mathcal{T}^0\big]^2$, it holds that*

$$\int_{\mathcal{E}_\mathcal{T}} [\![\Phi]\!] \{\mathbf{V}\} \le C_{\rm edge} \, \|[\![\Phi]\!]\|_{L_2(\mathcal{E}_\mathcal{T})} \, \|\mathbf{V}\|_{\mathbf{H}^{1/2}(\Gamma)} \,. \tag{3.4}$$

Furthermore, if $\widehat{\mathcal{T}}$ is the uniform refinement of $\mathcal{T}$ and $\widehat{\Phi} \in V_{\widehat{\mathcal{T}}}^0$, it holds that

$$\int_{\mathcal{E}_{\widehat{\mathcal{T}}}} \Big[\!\Big[\widehat{\Phi}\Big]\!\Big] \{\mathbf{V}\} \le C_{\rm edge} \, \Big\| h_\mathcal{T}^{1/2} (1 - \Pi_\mathcal{T}) \nabla_{\widehat{\mathcal{T}}} \widehat{\Phi} \Big\|_{\mathbf{L}_2(\Gamma)} \, \|\mathbf{V}\|_{\mathbf{H}^{1/2}(\Gamma)} \,. \tag{3.5}$$

Proof. For every edge $e \in \mathcal{E}_\mathcal{T}$, we use an affine map to transfer the edge patch ω_e to a reference configuration $\overline{\omega_e}$. As we emphasized in Section 2.2, the number of this reference configurations is bounded uniformly, which permits us to use scaling arguments. Now we choose $\mathbf{c}_e \in \mathbb{R}^2$ to be the mean value of $\overline{\mathbf{V}}$ on $\overline{e}$. A finite-dimension argument and a quotient-space argument, *cf.* [23], show

$$\big\| \overline{\mathbf{V}} - \mathbf{c}_e \big\|_{\mathbf{L}_2(\overline{e})} \lesssim \big| \overline{\mathbf{V}} \big|_{\mathbf{H}^{1/2}_{\rm slo}(\overline{\omega_e})} \,. \tag{3.6}$$

Mapping both sides back to the physical domain yields

$$\|\mathbf{V} - \mathbf{c}_e\|_{\mathbf{L}_2(e)} \lesssim |\mathbf{V}|_{\mathbf{H}^{1/2}_{\rm slo}(\omega_e)} \le \|\mathbf{V}\|_{\mathbf{H}^{1/2}_{\rm slo}(\omega_e)} \,. \tag{3.7}$$

As Φ is a Crouzeix–Raviart function, its jump $[\![\Phi]\!]$ has vanishing integral mean on every edge $e \in \mathcal{E}_\mathcal{T}$, and hence, using the Cauchy–Schwarz inequality, we obtain with (3.7)

$$\begin{aligned} \int_{\mathcal{E}_\mathcal{T}} [\![\Phi]\!] \{\mathbf{V}\} = \sum_{e \in \mathcal{E}_\mathcal{T}} \int_e [\![\Phi]\!] \{\mathbf{V} - \mathbf{c}_e\} &\le \left(\sum_{e \in \mathcal{E}_\mathcal{T}} \|[\![\Phi]\!]\|_{L_2(e)}^2 \right)^{1/2} \left(\sum_{e \in \mathcal{E}_\mathcal{T}} \|\mathbf{V} - \mathbf{c}_e\|_{\mathbf{L}_2(e)}^2 \right)^{1/2} \\ &\le \left(\sum_{e \in \mathcal{E}_\mathcal{T}} \|[\![\Phi]\!]\|_{L_2(e)}^2 \right)^{1/2} \left(\sum_{e \in \mathcal{E}_\mathcal{T}} \|\mathbf{V}\|_{\mathbf{H}^{1/2}_{\rm slo}(\omega_e)}^2 \right)^{1/2} . \end{aligned}$$

Locally, only three patches ω_e overlap. Therefore, the definition of the norm $\|\cdot\|_{H^{1/2}_{\rm slo}}$ and its equivalence with the interpolation norm on Γ conclude the proof of (3.4). Now we prove (3.5). We start at (3.4), this time with $\widehat{\mathcal{T}}$ instead of $\mathcal{T}$, to obtain

$$\int_{\mathcal{E}_{\widehat{\mathcal{T}}}} \Big[\!\Big[\widehat{\Phi}\Big]\!\Big] \{\mathbf{V}\} \lesssim \left(\sum_{e \in \mathcal{E}_{\widehat{\mathcal{T}}}} \Big\| \Big[\!\Big[\widehat{\Phi}\Big]\!\Big] \Big\|_{L_2(e)}^2 \right)^{1/2} \|\mathbf{V}\|_{\mathbf{H}^{1/2}(\Gamma)} \,.$$

Now we split the L_2 norm of the jump $\Big[\!\Big[\widehat{\Phi}\Big]\!\Big]$ over the skeleton $\mathcal{E}_{\widehat{\mathcal{T}}}$ into the contributions on the skeleton $\mathcal{E}_\mathcal{T}$ and the rest, which we write sloppy as $\mathcal{E}_{\widehat{\mathcal{T}}} \setminus \mathcal{E}_\mathcal{T}$. Then,

$$\sum_{e \in \mathcal{E}_{\widehat{\mathcal{T}}}} \Big\| \Big[\!\Big[\widehat{\Phi}\Big]\!\Big] \Big\|_{L_2(e)}^2 = \sum_{e \in \mathcal{E}_\mathcal{T}} \Big\| \Big[\!\Big[\widehat{\Phi}\Big]\!\Big] \Big\|_{L_2(e)}^2 + \sum_{e \in \mathcal{E}_{\widehat{\mathcal{T}}} \setminus \mathcal{E}_\mathcal{T}} \Big\| \Big[\!\Big[\widehat{\Phi}\Big]\!\Big] \Big\|_{L_2(e)}^2 \,. \tag{3.8}$$

We claim that there is a constant $C > 0$, independent of $\mathcal{E}_{\widehat{\mathcal{T}}}$ and $\widehat{\Phi}$ such that

$$\begin{aligned} \Big\| \Big[\!\Big[\widehat{\Phi}\Big]\!\Big] \Big\|_{L_2(e)} &\le C h_e^{1/2} \Big\| (1 - \Pi_\mathcal{T}) \nabla_{\widehat{\mathcal{T}}} \widehat{\Phi} \Big\|_{\mathbf{L}_2(\omega_e)} \qquad \text{if } e \in \mathcal{E}_\mathcal{T}, \\ \Big\| \Big[\!\Big[\widehat{\Phi}\Big]\!\Big] \Big\|_{L_2(e)} &\le C h_e^{1/2} \Big\| (1 - \Pi_\mathcal{T}) \nabla_{\widehat{\mathcal{T}}} \widehat{\Phi} \Big\|_{\mathbf{L}_2(T)} \qquad \text{if } e \in \mathcal{E}_{\widehat{\mathcal{T}}} \setminus \mathcal{E}_\mathcal{T} \text{ with } e \subset T \in \mathcal{T}. \end{aligned}$$

Both sides define seminorms, and the left one vanishes when the right one does. Hence, the bounded dimension of the underlying space and a scaling argument prove the claim. Using the last two estimates in (3.8) shows (3.5). □

Lemma 3.4. *In addition to Lemma 3.2, we have the following estimates, where $\widehat{\mathcal{T}}$ denotes the uniform refinement of $\mathcal{T}$: For $\Phi \in V_{\mathcal{T}}$ and $\widehat{\Phi} \in V_{\widehat{\mathcal{T}}}$, it holds that*

$$\|\nabla_{\mathcal{T}}(1 - I_{\mathcal{T}})\Phi\|_{\widetilde{\mathbf{H}}^{-1/2}(\Gamma)} \leq C_{\mathrm{I}} \left\|h_{\mathcal{T}}\, [\![\Phi]\!]'\right\|_{L_2(\mathcal{E}_{\mathcal{T}})}, \tag{3.9a}$$

$$\left\|\nabla_{\widehat{\mathcal{T}}}(1 - I_{\mathcal{T}})\widehat{\Phi}\right\|_{\widetilde{\mathbf{H}}^{-1/2}(\Gamma)} \leq C_{\mathrm{I}} \left\|h_{\mathcal{T}}^{1/2}(1 - \Pi_{\mathcal{T}})\nabla_{\widehat{\mathcal{T}}}\widehat{\Phi}\right\|_{\mathbf{L}_2(\Gamma)}. \tag{3.9b}$$

Proof. We will use estimates (3.2) and (3.3) to prove this lemma. First, if we denote by $I_{\mathcal{T}}\mathbf{v}$ the component-wise action of $I_{\mathcal{T}}$ to $\mathbf{v} \in \mathbf{H}^{1/2}(\Gamma)$, we integrate by parts piecewise to obtain

$$\langle \nabla_{\mathcal{T}}(1 - I_{\mathcal{T}})\Phi, I_{\mathcal{T}}\mathbf{v}\rangle = -\langle (1 - I_{\mathcal{T}})\Phi, \mathrm{div} I_{\mathcal{T}}\mathbf{v}\rangle + \sum_{T\in\mathcal{T}} \int_{\mathcal{E}_T} (\Phi - I_{\mathcal{T}}\Phi) I_{\mathcal{T}}\mathbf{v} \cdot \mathbf{n}_T.$$

As $[\![I_{\mathcal{T}}\Phi]\!]$ vanishes due to the continuity of $I_{\mathcal{T}}\Phi$, the second term on the right-hand side can be written as

$$\begin{aligned}\sum_{T\in\mathcal{T}} \int_{\mathcal{E}_T} (\Phi - I_{\mathcal{T}}\Phi) I_{\mathcal{T}}\mathbf{v} \cdot \mathbf{n}_T &= \int_{\mathcal{E}_{\mathcal{T}}} [\![\Phi - I_{\mathcal{T}}\Phi]\!]\, \{I_{\mathcal{T}}\mathbf{v}\} + \int_{\mathcal{E}_{\mathcal{T}}\setminus\partial\Gamma} \{\Phi - I_{\mathcal{T}}\Phi\}\, [\![I_{\mathcal{T}}\mathbf{v}]\!] \\ &= \int_{\mathcal{E}_{\mathcal{T}}} [\![\Phi]\!]\, \{I_{\mathcal{T}}\mathbf{v}\}.\end{aligned}$$

We conclude that, for any $\mathbf{v} \in \mathbf{H}^{1/2}(\Gamma)$,

$$\begin{aligned}\langle \nabla_{\mathcal{T}}(1 - I_{\mathcal{T}})\Phi, \mathbf{v}\rangle &= \langle \nabla_{\mathcal{T}}(1 - I_{\mathcal{T}})\Phi, \mathbf{v} - I_{\mathcal{T}}\mathbf{v}\rangle - \langle (1 - I_{\mathcal{T}})\Phi, \mathrm{div} I_{\mathcal{T}}\mathbf{v}\rangle \\ &\quad + \int_{\mathcal{E}_{\mathcal{T}}} [\![\Phi]\!]\, \{I_{\mathcal{T}}\mathbf{v}\}.\end{aligned} \tag{3.10}$$

We bound the terms on the right-hand side separately. Taking into account (3.3c), the first term on the right-hand side of (3.10) can be estimated by

$$\begin{aligned}\langle \nabla_{\mathcal{T}}(1 - I_{\mathcal{T}})\Phi, \mathbf{v} - I_{\mathcal{T}}\mathbf{v}\rangle &\leq \sum_{T\in\mathcal{T}} \|\nabla_{\mathcal{T}}(1 - I_{\mathcal{T}})\Phi\|_{\mathbf{L}_2(T)}\, \|\mathbf{v} - I_{\mathcal{T}}\mathbf{v}\|_{\mathbf{L}_2(T)} \\ &\lesssim \sum_{T\in\mathcal{T}} h_{\mathcal{T}}|_T^{-1/2}\, \|[\![\Phi]\!]\|_{L_2(\mathcal{E}_{\omega_T})}\, \|\mathbf{v} - I_{\mathcal{T}}\mathbf{v}\|_{\mathbf{L}_2(T)} \\ &\leq \|[\![\Phi]\!]\|_{L_2(\mathcal{E}_{\mathcal{T}})} \left\|h_{\mathcal{T}}^{-1/2}(\mathbf{v} - I_{\mathcal{T}}\mathbf{v})\right\|_{\mathbf{L}_2(\Gamma)}.\end{aligned} \tag{3.11}$$

Now, it holds that $\left\|h_{\mathcal{T}}^{-1/2}(\mathbf{v} - I_{\mathcal{T}}\mathbf{v})\right\|_{\mathbf{L}_2(\Gamma)} \lesssim \|\mathbf{v}\|_{\mathbf{H}^{1/2}(\Gamma)}$, which follows from interpolation of the estimates

$$\|\mathbf{v} - I_{\mathcal{T}}\mathbf{v}\|_{\mathbf{L}_2(\Gamma)} \lesssim \|\mathbf{v}\|_{\mathbf{L}_2(\Gamma)} \quad \text{and} \quad \left\|h_{\mathcal{T}}^{-1}(\mathbf{v} - I_{\mathcal{T}}\mathbf{v})\right\|_{\mathbf{L}_2(\Gamma)} \lesssim \|\mathbf{v}\|_{\mathbf{H}^1(\Gamma)},$$

which themselves can be derived summing (3.2) and (3.3a) over the elements of the mesh. We conclude that

$$\langle \nabla_{\mathcal{T}}(1 - I_{\mathcal{T}})\Phi, \mathbf{v} - I_{\mathcal{T}}\mathbf{v}\rangle \lesssim \|[\![\Phi]\!]\|_{L_2(\mathcal{E}_{\mathcal{T}})}\, \|\mathbf{v}\|_{\mathbf{H}^{1/2}(\Gamma)}. \tag{3.12}$$

The second contribution on the right-hand side of (3.10) can be bounded by using (3.3b) *via*

$$\begin{aligned}\langle \Phi - I_{\mathcal{T}}\Phi\,, \mathrm{div} I_{\mathcal{T}}\mathbf{v}\rangle &\leq \sum_{T\in\mathcal{T}} \|\Phi - I_{\mathcal{T}}\Phi\|_{L_2(T)}\, \|\mathrm{div} I_{\mathcal{T}}\mathbf{v}\|_{L_2(T)} \\ &\lesssim \|[\![\Phi]\!]\|_{L_2(\mathcal{E}_{\mathcal{T}})} \left\| h_{\mathcal{T}}^{1/2} \mathrm{div} I_{\mathcal{T}}\mathbf{v}\right\|_{L_2(\Gamma)} \\ &\lesssim \|[\![\Phi]\!]\|_{L_2(\mathcal{E}_{\mathcal{T}})}\, \|\mathbf{v}\|_{\mathbf{H}^{1/2}(\Gamma)}\,. \end{aligned} \tag{3.13}$$

In the last step we used an inverse estimate (*cf.* [10], Prop. 3.1) and the recent extension ([3], Prop. 5), and the fact that $I_{\mathcal{T}}$ is bounded in $\mathbf{H}^{1/2}(\Gamma)$, which again follows by interpolation, this time using the estimates (3.2). The third part on the right-hand side of (3.10) can be bounded by Lemma 3.3 and the $\mathbf{H}^{1/2}(\Gamma)$-boundedness of $I_{\mathcal{T}}$ *via*

$$\int_{\mathcal{E}_{\mathcal{T}}} [\![\Phi]\!]\, \{I_{\mathcal{T}}\mathbf{v}\} \lesssim \|[\![\Phi]\!]\|_{L_2(\mathcal{E}_{\mathcal{T}})}\, \|\mathbf{v}\|_{\mathbf{H}^{1/2}(\Gamma)}\,. \tag{3.14}$$

From the identity (3.10) we conclude, using (3.12)–(3.14), that

$$\|\nabla_{\mathcal{T}}(1-I_{\mathcal{T}})\Phi\|_{\tilde{\mathbf{H}}^{-1/2}(\Gamma)} = \sup_{\|\mathbf{v}\|_{\mathbf{H}^{1/2}(\Gamma)}=1} \langle \nabla_{\mathcal{T}}(1-I_{\mathcal{T}})\Phi\,, \mathbf{v}\rangle \lesssim \|[\![\Phi]\!]\|_{L_2(\mathcal{E}_{\mathcal{T}})}\,.$$

From this, (3.9a) follows from a Poincaré inequality, which may be used since $\Phi \in V_{\mathcal{T}}$ implies that the jump $[\![\Phi]\!]$ vanishes at the midpoint of every element.

To prove (3.9b), we again use integration by parts piecewise and conclude as before

$$\begin{aligned}\left\langle \nabla_{\widehat{\mathcal{T}}}(1-I_{\mathcal{T}})\widehat{\Phi}\,, \mathbf{v}\right\rangle &= \left\langle \nabla_{\widehat{\mathcal{T}}}(1-I_{\mathcal{T}})\widehat{\Phi}\,, \mathbf{v} - I_{\mathcal{T}}\mathbf{v}\right\rangle - \left\langle (1-I_{\mathcal{T}})\widehat{\Phi}\,, \mathrm{div} I_{\mathcal{T}}\mathbf{v}\right\rangle, \\ &\quad + \int_{\mathcal{E}_{\widehat{\mathcal{T}}}} \left[\!\!\left[\widehat{\Phi}\right]\!\!\right] \{I_{\mathcal{T}}\mathbf{v}\}. \end{aligned} \tag{3.15}$$

The first and second term can be bounded as in (3.11) and (3.13), this time using the local estimates

$$\begin{aligned}\left\|\nabla_{\widehat{\mathcal{T}}}(1-I_{\mathcal{T}})\widehat{\Phi}\right\|_{\mathbf{L}_2(T)} &\leq C \left\|(1-\Pi_{\mathcal{T}})\nabla_{\widehat{\mathcal{T}}}\widehat{\Phi}\right\|_{\mathbf{L}_2(\omega_T)} \\ \left\|(1-I_{\mathcal{T}})\widehat{\Phi}\right\|_{L_2(T)} &\leq C h_{\mathcal{T}}|_T \left\|(1-\Pi_{\mathcal{T}})\nabla_{\widehat{\mathcal{T}}}\widehat{\Phi}\right\|_{\mathbf{L}_2(\omega_T)}, \end{aligned}$$

which follow from a scaling argument and norm equivalence in finite dimensional spaces. The last term in (3.15) can be bounded by (3.5) of Lemma 3.3. □

We will also need the following boundedness result for $I_{\mathcal{T}}$.

Lemma 3.5. *In addition to Lemma 3.2, we have the following estimate, where $\widehat{\mathcal{T}}$ denotes the uniform refinement of $\mathcal{T}$: For $\Phi \in V_{\mathcal{T}}$ and $\widehat{\Phi} \in V_{\widehat{\mathcal{T}}}$, it holds that*

$$\left\|\nabla_{\mathcal{T}} I_{\mathcal{T}}\widehat{\Phi}\right\|_{\tilde{\mathbf{H}}^{-1/2}(\Gamma)} \leq C_{\mathrm{I}} \left\|\nabla_{\widehat{\mathcal{T}}}\widehat{\Phi}\right\|_{\tilde{\mathbf{H}}^{-1/2}(\Gamma)}. \tag{3.16}$$

Proof. To prove (3.16), we first observe that due to the local L_2 boundedness of $(1-\Pi_{\mathcal{T}})$ and the inverse estimate ([21], Thm. 3.6), we have

$$\left\|h_{\mathcal{T}}^{1/2}(1-\Pi_{\mathcal{T}})\nabla_{\widehat{\mathcal{T}}}\widehat{\Phi}\right\|_{\mathbf{L}_2(\Gamma)} \leq \left\|h_{\mathcal{T}}^{1/2}\nabla_{\widehat{\mathcal{T}}}\widehat{\Phi}\right\|_{\mathbf{L}_2(\Gamma)} \lesssim \left\|\nabla_{\widehat{\mathcal{T}}}\widehat{\Phi}\right\|_{\tilde{\mathbf{H}}^{-1/2}(\Gamma)}.$$

Hence, the triangle inequality and (3.9b) show

$$\left\|\nabla_{\widehat{\mathcal{T}}} I_{\mathcal{T}}\widehat{\Phi}\right\|_{\tilde{\mathbf{H}}^{-1/2}(\Gamma)} \leq \left\|\nabla_{\widehat{\mathcal{T}}}\widehat{\Phi}\right\|_{\tilde{\mathbf{H}}^{-1/2}(\Gamma)} + \left\|\nabla_{\widehat{\mathcal{T}}}(1-I_{\mathcal{T}})\widehat{\Phi}\right\|_{\tilde{\mathbf{H}}^{-1/2}(\Gamma)} \lesssim \left\|\nabla_{\widehat{\mathcal{T}}}\widehat{\Phi}\right\|_{\tilde{\mathbf{H}}^{-1/2}(\Gamma)}.$$

□

4. *A posteriori* error estimation and adaptive algorithm

In this section, we introduce different error estimators, and show their reliability and efficiency. In Section 4.1, we introduce global error estimators, that is, the employed (non-integer) norm is nonlocal and therefore does not provide information for local mesh-refinement. In Section 4.2, we pass over to weighted (integer) norms, which are local and can therefore be employed in an adaptive algorithm, which will be introduced in Section 4.3. In order to estimate the nonconformity of a function in terms of the function itself, we will use the results of Sections 3.1 and 3.2.

Corollary 4.1. *Denote by $\mathcal{T}$ a refinement of $\mathcal{T}_0$. Let $\Phi \in V_{\mathcal{T}}$ be the Galerkin solution (2.4). Then, there is a constant $C_4 > 0$ which depends only on $\mathcal{T}_0$ such that*

$$\left|\!\left|\!\left|\Phi^\perp\right|\!\right|\!\right|_{\mathcal{T}} = \left|\!\left|\!\left|\Phi - \Phi^0\right|\!\right|\!\right|_{\mathcal{T}} \leq C_4 \left\| h_{\mathcal{T}} \, [\![\Phi]\!]' \right\|_{L_2(\mathcal{E}_{\mathcal{T}})}.$$

Proof. This follows easily by using the fact that $\Phi - \Phi^0$ is $a_{\mathcal{T}}$-orthogonal to $V_{\mathcal{T}}^0$ and employing (3.9a). □

4.1. Global error estimators

Let $\Phi \in V_{\mathcal{T}}$ and $\widehat{\Phi} \in V_{\widehat{\mathcal{T}}}$ be Galerkin solutions (2.4), where $\widehat{\mathcal{T}}$ is a uniform refinement of $\mathcal{T}$. We introduce estimators on the mesh $\mathcal{T}$ by

$$\eta_{\mathcal{T}} := \left|\!\left|\!\left|\widehat{\Phi} - \Phi\right|\!\right|\!\right|_{\widehat{\mathcal{T}}} = \left\| \mathbf{curl}_{\widehat{\mathcal{T}}}(\widehat{\Phi} - \Phi) \right\|_{\widetilde{\mathbf{H}}^{-1/2}(\Gamma)},$$
$$\widetilde{\eta}_{\mathcal{T}} := \left|\!\left|\!\left|\widehat{\Phi} - I_{\mathcal{T}}\widehat{\Phi}\right|\!\right|\!\right|_{\widehat{\mathcal{T}}} = \left\| \mathbf{curl}_{\widehat{\mathcal{T}}}(\widehat{\Phi} - I_{\mathcal{T}}\widehat{\Phi}) \right\|_{\widetilde{\mathbf{H}}^{-1/2}(\Gamma)}.$$

The existing derivations of $h - h/2$ error estimators, *e.g.* [16,18], focus on conforming methods and rely mostly on the Galerkin orthogonality (1.3). Contrary, we have the weaker partial orthogonality of Lemma 3.1, where additional terms arise (what we called nonconformity error) which account for the nonconformity. In Corollary 4.1, we showed that these terms can be bounded by the inter-element jumps of Φ, *i.e.*, by

$$\rho_{\mathcal{T}} := \left\| h_{\mathcal{T}} \, [\![\Phi]\!]' \right\|_{L_2(\mathcal{E}_{\mathcal{T}})}.$$

Consequently, we have that $\eta_{\mathcal{T}}$ and $\widetilde{\eta}_{\mathcal{T}}$ are equivalent up to $\rho_{\mathcal{T}}$.

Lemma 4.2. *Let $\mathcal{T}$ be a refinement of $\mathcal{T}_0$. Then, there is a constant $C_5 > 0$ which depends only on $\mathcal{T}_0$ such that*

$$C_5^{-1} \left|\!\left|\!\left|\widehat{\Phi} - \Phi\right|\!\right|\!\right|_{\widehat{\mathcal{T}}} \leq \left|\!\left|\!\left|\widehat{\Phi} - I_{\mathcal{T}}\widehat{\Phi}\right|\!\right|\!\right|_{\widehat{\mathcal{T}}} + \rho_{\mathcal{T}} \quad \text{and} \quad C_5^{-1} \left|\!\left|\!\left|\widehat{\Phi} - I_{\mathcal{T}}\widehat{\Phi}\right|\!\right|\!\right|_{\widehat{\mathcal{T}}} \leq \left|\!\left|\!\left|\widehat{\Phi} - \Phi\right|\!\right|\!\right|_{\widehat{\mathcal{T}}} + \rho_{\mathcal{T}}.$$

Proof. As $\widehat{\Phi} - \Phi$ is orthogonal to $V_{\mathcal{T}}^0$ in $a_{\widehat{\mathcal{T}}}$, we conclude

$$\left|\!\left|\!\left|\widehat{\Phi} - \Phi\right|\!\right|\!\right|_{\widehat{\mathcal{T}}} \lesssim \left|\!\left|\!\left|\widehat{\Phi} - \Phi + \Phi^0 - I_{\mathcal{T}}\widehat{\Phi}\right|\!\right|\!\right| \leq \left|\!\left|\!\left|\widehat{\Phi} - I_{\mathcal{T}}\widehat{\Phi}\right|\!\right|\!\right|_{\widehat{\mathcal{T}}} + \left|\!\left|\!\left|\Phi - \Phi^0\right|\!\right|\!\right|_{\mathcal{T}},$$

and the last term can be bounded by $\rho_{\mathcal{T}}$ by Corollary 4.1. To see the second estimate, we use the projection property and boundedness (3.16) of $I_{\mathcal{T}}$ to see that

$$\left|\!\left|\!\left|\widehat{\Phi} - I_{\mathcal{T}}\widehat{\Phi}\right|\!\right|\!\right|_{\widehat{\mathcal{T}}} \lesssim \left|\!\left|\!\left|\widehat{\Phi} - \Phi^0\right|\!\right|\!\right|_{\widehat{\mathcal{T}}} \leq \left|\!\left|\!\left|\widehat{\Phi} - \Phi\right|\!\right|\!\right|_{\widehat{\mathcal{T}}} + \left|\!\left|\!\left|\Phi - \Phi^0\right|\!\right|\!\right|_{\mathcal{T}},$$

which shows the desired estimate. □

In a next step, we show the efficiency and reliability of $\eta_{\mathcal{T}}$. For the reliability, we assume that a saturation assumption for the *conforming* approximations holds true.

Theorem 4.3. *Let $\mathcal{T}$ be a refinement of $\mathcal{T}_0$. Then, there is a constant $C_{\rm eff} > 0$ such that $\eta_{\mathcal{T}} = \left|\!\left|\!\left|\widehat{\Phi} - \Phi\right|\!\right|\!\right|_{\widehat{\mathcal{T}}}$ is efficient up to the nonconformity error,* i.e.*,*

$$C_{\rm eff}^{-1} \left|\!\left|\!\left|\widehat{\Phi} - \Phi\right|\!\right|\!\right|_{\widehat{\mathcal{T}}} \le |||\phi - \Phi|||_{\mathcal{T}} + \rho_{\mathcal{T}} + \rho_{\widehat{\mathcal{T}}}. \tag{4.1}$$

Furthermore, assume that there is a constant $C_{\rm sat} \in (0,1)$ such that the saturation assumption for the conforming approximations

$$a_{\widehat{\mathcal{T}}}\left(\phi - \widehat{\Phi}^0, \phi - \widehat{\Phi}^0\right) \le C_{\rm sat} a_{\mathcal{T}}\left(\phi - \Phi^0, \phi - \Phi^0\right) \tag{4.2}$$

holds true. Then, there is a constant $C_{\rm rel} > 0$ such that $\eta_{\mathcal{T}} = \left|\!\left|\!\left|\widehat{\Phi} - \Phi\right|\!\right|\!\right|_{\widehat{\mathcal{T}}}$ is reliable up to $\rho_{\mathcal{T}} + \rho_{\widehat{\mathcal{T}}}$, i.e.*,*

$$C_{\rm rel}^{-1} |||\phi - \Phi|||_{\mathcal{T}} \le \left|\!\left|\!\left|\widehat{\Phi} - \Phi\right|\!\right|\!\right|_{\widehat{\mathcal{T}}} + \rho_{\mathcal{T}} + \rho_{\widehat{\mathcal{T}}} \tag{4.3}$$

holds true.

Proof. Efficiency (4.1) follows immediately from Lemma 3.1 by setting $\mathcal{T}_\star := \widehat{\mathcal{T}}$ and Corollary 4.1.

To show reliability (4.3), we first note that the triangle inequality and ellipticity give

$$|||\phi - \Phi||| \lesssim a\left(\phi - \Phi^0, \phi - \Phi^0\right) + \rho_{\mathcal{T}}.$$

Now, due to the conforming orthogonality and the saturation assumption (4.2),

$$\begin{aligned}(1 - C_{\rm sat}) a\left(\phi - \Phi^0, \phi - \Phi^0\right) &\le a\left(\Phi^0 - \widehat{\Phi}^0, \Phi^0 - \widehat{\Phi}^0\right) \lesssim \left|\!\left|\!\left|\Phi^0 - \widehat{\Phi}^0\right|\!\right|\!\right|_{\widehat{\mathcal{T}}} \\ &\le \left|\!\left|\!\left|\widehat{\Phi} - \Phi\right|\!\right|\!\right|_{\widehat{\mathcal{T}}} + |||\Phi - \Phi^0||| + \left|\!\left|\!\left|\widehat{\Phi} - \widehat{\Phi}^0\right|\!\right|\!\right| \\ &\lesssim \left|\!\left|\!\left|\widehat{\Phi} - \Phi\right|\!\right|\!\right|_{\widehat{\mathcal{T}}} + \rho_{\mathcal{T}} + \rho_{\widehat{\mathcal{T}}},\end{aligned}$$

where we used the triangle inequality and Corollary 4.1. □

Remark 4.4. In finite element methods, the saturation assumption (4.2) is verified for the Poisson problem $-\Delta u = f$. In fact, in [15] it is shown that

$$\left|\!\left|\!\left|\phi - \widehat{\Phi}_\ell^0\right|\!\right|\!\right| \le C_{\rm sat} |||\phi - \Phi_\ell^0||| + {\rm osc}_\ell,$$

where ${\rm osc}_\ell$ is a measure for the resolution of f on the mesh $\mathcal{T}_\ell$. Hence, small data oscillation implies the saturation assumption. However, the saturation assumption (4.2) is not proven for BEM. To the best of the our knowledge, the only contributions are [2,17]. In [2], it is shown that for $2D$-BEM for the weakly singular integral equation, there is a $k \in \mathbb{N}$ and $C_{\rm sat} < 1$ which depend only on $\mathcal{T}_0$ and Γ, such that with k uniform refinements of $\mathcal{T}_\ell$, which we denote by $\mathcal{T}_{\ell(k)}$, there holds

$$|||\phi - \Phi_\ell||| \le C_{\rm sat} \left|\!\left|\!\left|\phi - \Phi_{\ell(k)}\right|\!\right|\!\right| + {\rm osc}_\ell$$

with ${\rm osc}_\ell$ being a term of higher order than the others. In [17], the saturation assumption is analyzed for an edge singularity on a plane square-shaped domain, and uniform as well as graded meshes are considered.

4.2. Localized error estimators

The *a posteriori* estimators of Section 4.1 use the $\widetilde{\mathbf{H}}^{-1/2}(\Gamma)$-norm, which is hard to compute and nonlocal. In order to provide *a posteriori* error estimators which can be split into element-wise indicators, we will use a weighted $\mathbf{L}_2$-norm. We introduce the localized estimators

$$\mu_{\mathcal{T}} := \left\| h_{\mathcal{T}}^{1/2} \mathbf{curl}_{\widehat{\mathcal{T}}} (\widehat{\Phi} - \Phi) \right\|_{\mathbf{L}_2(\Gamma)},$$
$$\widetilde{\mu}_{\mathcal{T}} := \left\| h_{\mathcal{T}}^{1/2} \left(\mathbf{curl}_{\widehat{\mathcal{T}}} \widehat{\Phi} - \Pi_{\mathcal{T}} \mathbf{curl}_{\widehat{\mathcal{T}}} \widehat{\Phi} \right) \right\|_{\mathbf{L}_2(\Gamma)}.$$

Splitting a nonlocal estimator (like $\eta_{\mathcal{T}}$) into a localized estimator (like $\widetilde{\mu}_{\mathcal{T}}$) is not a peculiarity of *a posteriori* error estimation in boundary elements. For example, the residual of a standard finite element approximation for, *e.g.*, the Poisson equation, is measured in the non-local norm of H^{-1}, but well-known residual error estimates consider the residual in a weighted L_2 norm (which is localized), *cf.* [32]. For results on the $h - h/2$ strategy in finite element methods (even convergence of adaptive algorithms), we refer to ([19], Sect. 2). We have the following result on efficiency and reliability.

Theorem 4.5. *There holds*

$$\left\| h_{\mathcal{T}}^{1/2} \left(\mathbf{curl}_{\widehat{\mathcal{T}}} \widehat{\Phi} - \Pi_{\mathcal{T}} \mathbf{curl}_{\widehat{\mathcal{T}}} \widehat{\Phi} \right) \right\|_{\mathbf{L}_2(\Gamma)} \leq \left\| h_{\mathcal{T}}^{1/2} \mathbf{curl}_{\widehat{\mathcal{T}}} \left(\widehat{\Phi} - \Phi \right) \right\|_{\mathbf{L}_2(\Gamma)} \lesssim \left| \left| \left| \widehat{\Phi} - \Phi \right| \right| \right|_{\widehat{\mathcal{T}}} \tag{4.4a}$$

and

$$\left| \left| \left| \widehat{\Phi} - I_{\mathcal{T}} \widehat{\Phi} \right| \right| \right|_{\widehat{\mathcal{T}}} \lesssim \left\| h_{\mathcal{T}}^{1/2} \left(\mathbf{curl}_{\widehat{\mathcal{T}}} \widehat{\Phi} - \Pi_{\mathcal{T}} \mathbf{curl}_{\widehat{\mathcal{T}}} \widehat{\Phi} \right) \right\|_{\mathbf{L}_2(\Gamma)}. \tag{4.4b}$$

In particular, all estimators are equivalent up to $\rho_{\mathcal{T}} + \rho_{\widehat{\mathcal{T}}}$*, and for* $\tau \in \{\eta_{\mathcal{T}}, \widetilde{\eta}_{\mathcal{T}}, \mu_{\mathcal{T}}, \widetilde{\mu}_{\mathcal{T}}\}$*, the estimator* τ *is efficient up to* $\rho_{\mathcal{T}} + \rho_{\widehat{\mathcal{T}}}$*, and under the saturation assumption* (4.2) *for the conforming approximations it is also reliable,* i.e.*,*

$$|||\phi - \Phi||| \lesssim \tau + \rho_{\mathcal{T}} + \rho_{\widehat{\mathcal{T}}},$$
$$\tau \lesssim |||\phi - \Phi||| + \rho_{\mathcal{T}} + \rho_{\widehat{\mathcal{T}}}.$$

Proof. As in [18], the first estimate in (4.4a) follows from the best approximation property of $\Pi_{\mathcal{T}}$, while the second one follows from the inverse inequality ([21], Thm. 3.6). The first estimate in (4.4b) is estimate (3.9b) from Lemma 3.4. Now, since

$$\eta_{\mathcal{T}} = \left| \left| \left| \widehat{\Phi} - \Phi \right| \right| \right|_{\widehat{\mathcal{T}}} \quad \text{and} \quad \widetilde{\eta}_{\mathcal{T}} = \left| \left| \left| \widehat{\Phi} - I_{\mathcal{T}} \widehat{\Phi} \right| \right| \right|_{\widehat{\mathcal{T}}}$$

are equivalent up to $\rho_{\mathcal{T}} + \rho_{\widehat{\mathcal{T}}}$ according to Lemma 4.2, all estimators are equivalent up to $\rho_{\mathcal{T}} + \rho_{\widehat{\mathcal{T}}}$ as well. As $\eta_{\mathcal{T}}$ is efficient and reliable (given the saturation (4.2)) up to $\rho_{\mathcal{T}} + \rho_{\widehat{\mathcal{T}}}$ according to Theorem 4.3, this is also true for the three other estimators. □

4.3. Statement of the adaptive algorithm

We now introduce two adaptive algorithms. As error indicators on a mesh $\mathcal{T}_\ell$, we use the element-wise quantities $\widetilde{\mu}_\ell$, ρ_ℓ, and $\widehat{\rho}_\ell$. The first adaptive algorithm uses on every element $T \in \mathcal{T}_\ell$ the combined quantity

$$\sigma_\ell(T)^2 := \widetilde{\mu}_\ell(T)^2 + \rho_\ell(T)^2 + \widehat{\rho}_\ell(T)^2$$
$$:= \left\| h_\ell^{1/2} (1 - \Pi_\ell) \mathbf{curl}_{\widehat{\mathcal{T}}_\ell} \widehat{\Phi}_\ell \right\|_{\mathbf{L}_2(T)}^2 + \left\| h_\ell \left[\!\left[\Phi_\ell \right]\!\right]' \right\|_{L_2(\mathcal{E}_\ell(T))}^2 + \left\| \widehat{h}_\ell \left[\!\left[\widehat{\Phi}_\ell \right]\!\right]' \right\|_{L_2(\widehat{\mathcal{E}}_\ell(T))}^2.$$

For a subset $\mathcal{M}_\ell \subset \mathcal{T}_\ell$, we write

$$\begin{aligned}\sigma_\ell(\mathcal{M}_\ell)^2 &:= \widetilde{\mu}_\ell(\mathcal{M}_\ell)^2 + \rho_\ell(\mathcal{M}_\ell)^2 + \widehat{\rho}_\ell(\mathcal{M}_\ell)^2 \\ &:= \sum_{T\in\mathcal{M}_\ell} \widetilde{\mu}_\ell(T)^2 + \sum_{T\in\mathcal{M}_\ell} \rho_\ell(T)^2 + \sum_{T\in\mathcal{M}_\ell} \widehat{\rho}_\ell(T)^2\end{aligned}$$

and we use the abbreviations $\sigma_\ell := \sigma_\ell(\mathcal{T}_\ell)$, $\rho_\ell := \rho_\ell(\mathcal{T}_\ell)$, and $\widehat{\rho}_\ell := \widehat{\rho}_\ell(\mathcal{T}_\ell)$. Hence,

$$\sigma_\ell^2 = \widetilde{\mu}_\ell^2 + \rho_\ell^2 + \widehat{\rho}_\ell^2$$

is a reliable error estimator according to Theorem 4.5. The first adaptive algorithm now reads as follows.

Algorithm 1. Input: Initial mesh $\mathcal{T}_0$, parameter $\theta \in (0,1)$, counter $\ell := 0$.

(i) Obtain $\widehat{\mathcal{T}}_\ell$ by uniform bisec(3)-refinement of $\mathcal{T}_\ell$, see Figure 1.
(ii) Compute solutions Φ_ℓ and $\widehat{\Phi}_\ell$ of (2.4) with respect to $\mathcal{T}_\ell$ and $\widehat{\mathcal{T}}_\ell$.
(iii) Compute refinement indicators $\sigma_\ell(T)$ for all $T \in \mathcal{T}_\ell$.
(iv) Choose a set $\mathcal{M}_\ell \subseteq \mathcal{T}_\ell$ with minimal cardinality such that

$$\sum_{T\in\mathcal{M}_\ell} \sigma_\ell(T)^2 \geq \theta \sum_{T\in\mathcal{T}_\ell} \sigma_\ell(T)^2. \tag{4.5}$$

(v) Refine mesh $\mathcal{T}_\ell$ according to Algorithm NVB and obtain $\mathcal{T}_{\ell+1}$.
(vi) Update counter $\ell := \ell + 1$ and goto (i).

The marking strategy (4.5) uses the combined quantity σ_ℓ to single out elements for refinement. In this form, it was used in the pioneering work [14] to show convergence of an adaptive finite element scheme. In the presence of data oscillations, one can also use a *separated* marking strategy as it was used in [30] to prove optimality of an adaptive finite element scheme. The adaptive algorithm then looks as follows.

Algorithm 2. Input: Initial mesh $\mathcal{T}_0$, parameters $\theta_1, \theta_2, \vartheta \in (0,1)$, counter $\ell := 0$.

(i) Obtain $\widehat{\mathcal{T}}_\ell$ by uniform bisec(3)-refinement of $\mathcal{T}_\ell$, see Figure 1.
(ii) Compute solutions Φ_ℓ and $\widehat{\Phi}_\ell$ of (2.4) with respect to $\mathcal{T}_\ell$ and $\widehat{\mathcal{T}}_\ell$.
(iii) Compute refinement indicators $\sigma_\ell(T)$ for all $T \in \mathcal{T}_\ell$.
(iv) In case that $\rho_\ell^2 + \widehat{\rho}_\ell^2 \leq \vartheta \widetilde{\mu}_\ell^2$ choose a set $\mathcal{M}_\ell \subseteq \mathcal{T}_\ell$ with minimal cardinality such that

$$\sum_{T\in\mathcal{M}_\ell} \widetilde{\mu}_\ell(T)^2 \geq \theta_1 \sum_{T\in\mathcal{T}_\ell} \widetilde{\mu}_\ell(T)^2. \tag{4.6a}$$

In case that $\rho_\ell^2 + \widehat{\rho}_\ell^2 > \vartheta \widetilde{\mu}_\ell^2$ choose a set $\mathcal{M}_\ell \subseteq \mathcal{T}_\ell$ with minimal cardinality such that

$$\sum_{T\in\mathcal{M}_\ell} \left(\rho_\ell(T)^2 + \widehat{\rho}_\ell(T)^2\right) \geq \theta_2 \sum_{T\in\mathcal{T}_\ell} \left(\rho_\ell(T)^2 + \widehat{\rho}_\ell(T)^2\right). \tag{4.6b}$$

(v) Refine mesh $\mathcal{T}_\ell$ according to Algorithm NVB and obtain $\mathcal{T}_{\ell+1}$.
(vi) Update counter $\ell := \ell + 1$ and goto (i).

It can be easily seen that the separated marking strategy (4.6a)–(4.6b) implies the combined strategy (4.5) (with different parameter θ, though).

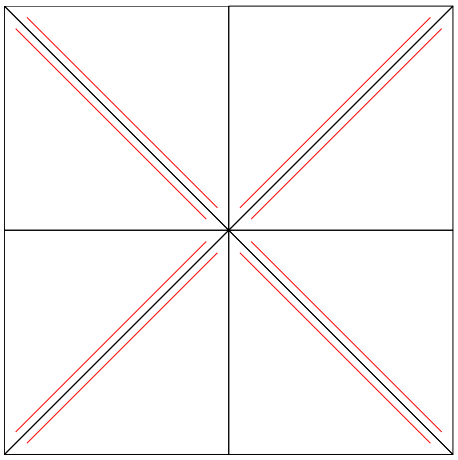

FIGURE 3. Initial mesh $\mathcal{T}_0$ used in the numerical experiments.

5. Numerical experiments

In this section we present numerical experiments for two different problems. The exact solution ϕ of the first experiment will be *smooth* in the sense that uniform and adaptive mesh refinement yield the same rate of convergence. Still, ϕ exhibits singularities which stem from the geometric setting (*i.e.*, polygonal boundary). As we emphasized in the introduction, it is a peculiarity of Crouzeix–Raviart BEM that uniform mesh refinement is optimal for these kind of singularities.

The second example reports on a case where the right-hand side of our model problem is chosen to be singular, such that, due to the mapping properties of $\mathcal{W}$, the exact solution ϕ suffers from low regularity as well. In this case, it will turn out that uniform mesh-refinement is suboptimal while adaptive refinement recovers the optimal rate.

5.1. Experiment with geometrically inherent singularities

We consider the screen $\Gamma := [0,1]^2$. The initial mesh $\mathcal{T}_0$ consists of 8 congruent triangles (*cf.* Fig. 3), such that Γ is halved along the diagonals and the midpoints of its sides. The reference edges are chosen on the two diagonals. The right-hand side is given by

$$f(x,y) = 1,$$

and it is well-known that the exact solution ϕ has square root edge singularities [28] so that $\phi \in \widetilde{H}^{1-\varepsilon}(\Gamma)$ for all $\varepsilon > 0$. As the regularity is known, the energy error $|||\phi|||$ can be approximated by extrapolation. We use the following sequences of meshes.

Uniform sequence

The sequence $\mathcal{T}_\ell$, $\ell \in \mathbb{N}_0$, is generated by uniform refinement, *i.e.*, the initial mesh $\mathcal{T}_0$ is chosen as in Figure 3, and the mesh $\mathcal{T}_\ell$, $\ell \geq 1$ is generated from $\mathcal{T}_{\ell-1}$ by a bisec(3)-refinement (as described in Fig. 1) of every triangle $T \in \mathcal{T}_\ell$. Due to the results in [24], we expect a convergence rate of $\mathcal{O}(h_\ell^{1/2-\varepsilon}) = \mathcal{O}(N_\ell^{-1/4+\varepsilon})$ for all $\varepsilon > 0$, *cf.* (2.5). This is exactly what we observe in the convergence history in Figure 4.

Adaptive sequence

The sequence of meshes $\mathcal{T}_\ell$, $\ell \in \mathbb{N}_0$, is generated by Algorithms 1 and 2, where $\mathcal{T}_0$ is chosen as in Figure 3. As we conjectured in Section 2.4, the rate $\mathcal{O}(N_\ell^{-1/4})$ cannot be improved in general, and this is what we see

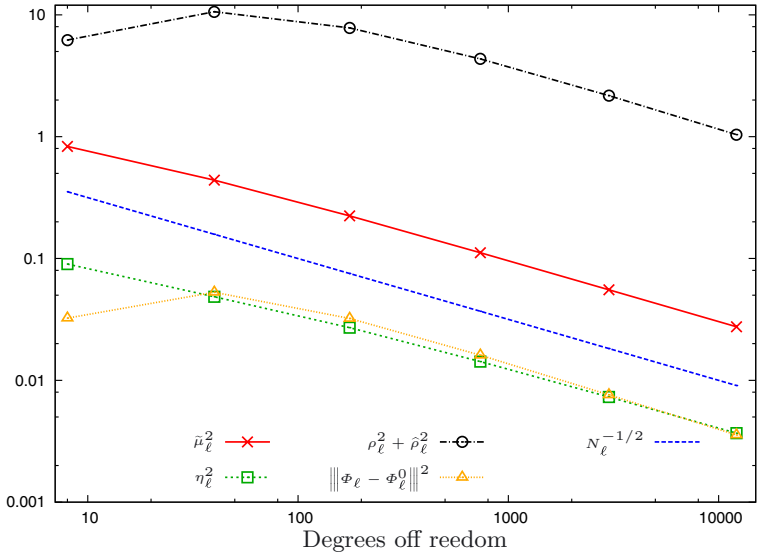

FIGURE 4. Convergence history for uniform mesh refinement and geometric singularities. The squared quantities exhibit the optimal rate $\mathcal{O}(N_\ell^{-1/2})$.

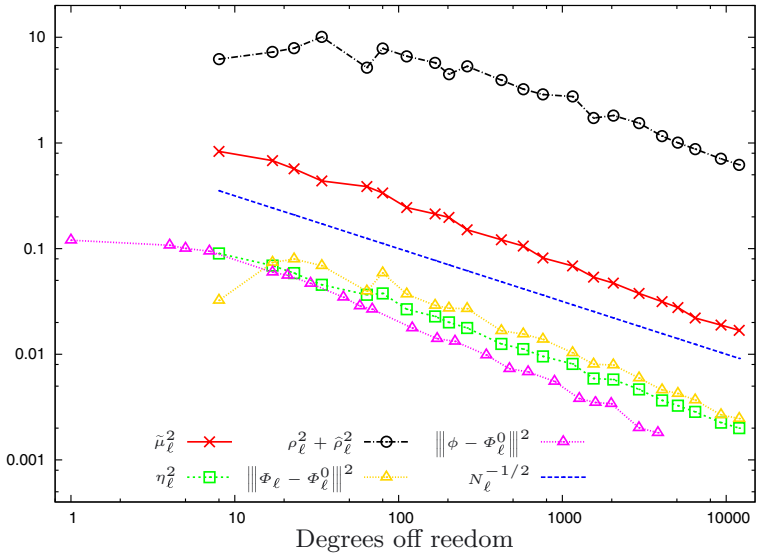

FIGURE 5. Convergence history for adaptive Algorithm 1 with $\theta = 0.5$ and geometric singularities. The squared quantities exhibit the optimal rate $\mathcal{O}(N_\ell^{-1/2})$.

in the experimental results. Figure 5 shows the convergence history of Algorithm 1 with $\theta = 0.5$, and we see that all involved quantities are of order $\mathcal{O}(N_\ell^{-1/4})$ (note that we plot squared quantities). In Figure 11 we plot the intermediate mesh $\mathcal{T}_{11}$ and the final mesh $\mathcal{T}_{21}$ that are constructed by the adaptive algorithm. What we observe qualitatively is that the meshes are refined towards the boundary $\partial\Gamma$, which meets the expectation as ϕ exhibits singularities there. Nevertheless, the computed meshes are not optimal for a conforming method. This is visualized in Figure 5, where we also plot the conforming energy error $|||\phi - \Phi_\ell^0|||^2$. Clearly, we use the number of the degrees of freedom of the conforming method for the x-axis. The previous choice $\theta = 0.5$ is arbitrary;

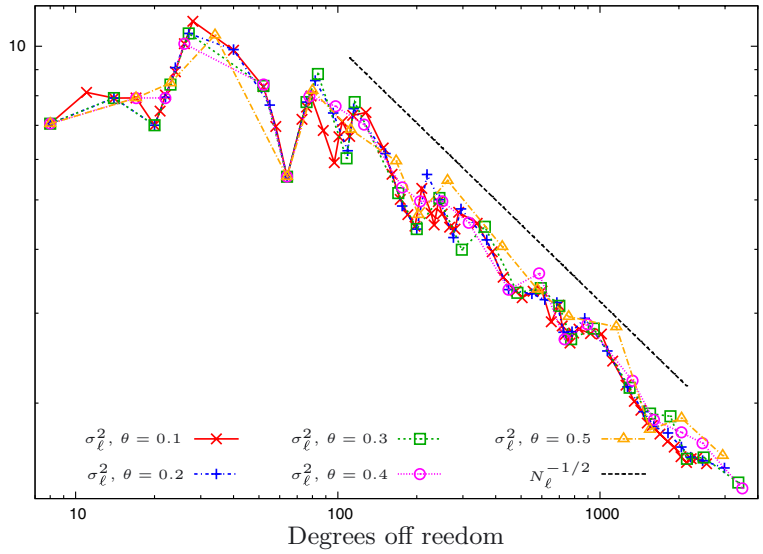

FIGURE 6. Error estimator σ_ℓ^2 for adaptive Algorithm 1 and geometric singularities with different values of $\theta \in \{0.1, 0.2, 0.3, 0.4, 0.5\}$. The squared quantities exhibit the optimal rate $\mathcal{O}(N_\ell^{-1/2})$ for all given choices of θ.

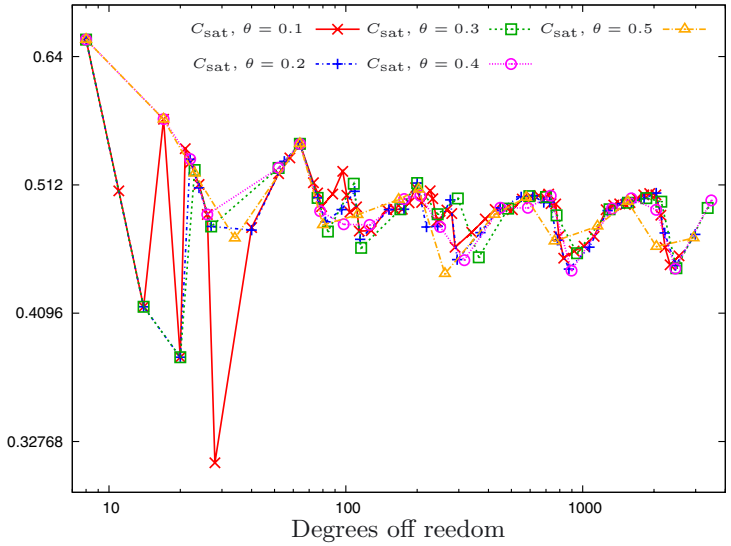

FIGURE 7. Saturation constants $C_{\rm sat}$ for adaptive Algorithm 1 and geometric singularities with different values of $\theta \in \{0.1, 0.2, 0.3, 0.4, 0.5\}$.

contemporary analysis of adaptive algorithms requires the parameter θ to be small enough in order to ensure optimal convergence. In Figure 6 we therefore plot the error estimate σ_ℓ^2 produced by Algorithm 1 for choices $\theta \in \{0.1, 0.2, 0, 3, 0.4, 0.5\}$. All choices produce the same qualitative results. As already said, the energy error of the solution can be extrapolated well in this case. For the conforming solutions Φ^0 and $\widehat{\Phi}^0$ we have Galerkin orthogonality in the energy norm, and so we are able to compute the saturation constant $C_{\rm sat}$ from (4.2). The assumption $C_{\rm sat} < 1$ implies reliability of our error estimator. In Figure 7, we plot the values of $C_{\rm sat}$ for the

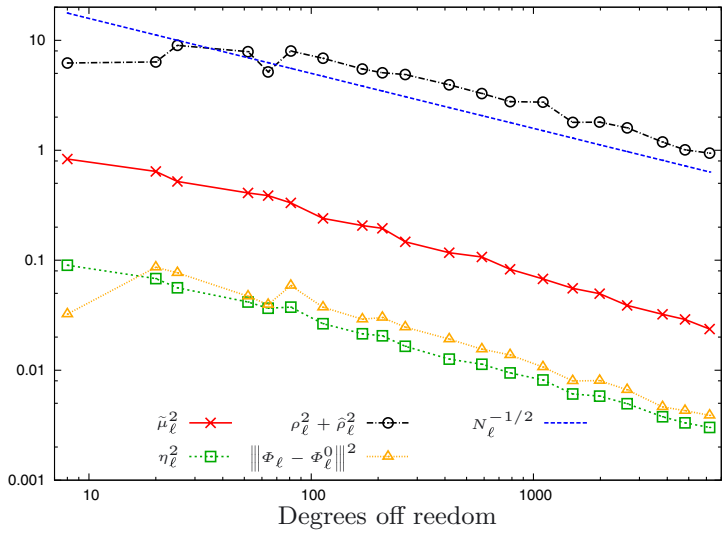

FIGURE 8. Convergence history for adaptive Algorithm 2 with separate marking and geometric singularities. The squared quantities exhibit the optimal rate $\mathcal{O}(N_\ell^{-1/2})$.

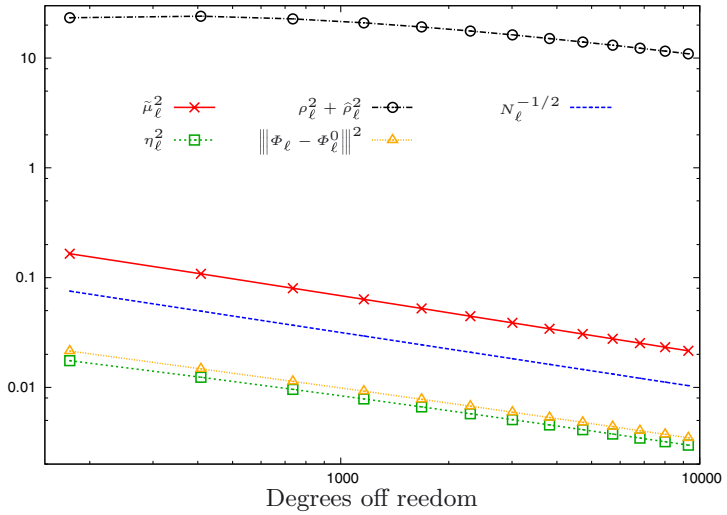

FIGURE 9. Convergence history for graded meshes with $\beta = 2$ and geometric singularities. The squared quantities exhibit the optimal rate $\mathcal{O}(N_\ell^{-1/2})$.

adaptive Algorithm 1 with different values of θ. We observe that $C_{\mathrm{sat}} < 1$ uniformly for all choices of θ. Finally, we present the outcome of Algorithm 2 with the choice $\theta_1 = \theta_2 = \vartheta = 0.5$ in Figure 8. As the jumps ρ_ℓ and $\widehat{\rho}_\ell$ dominate the estimator $\widetilde{\mu}_\ell$ by one order of magnitude, Algorithm 2 will use only the marking strategy (4.6b). Again, the order of convergence is $\mathcal{O}(N_\ell^{-1/4})$ as expected.

Graded sequence

We use a sequence of meshes $\mathcal{T}_\ell$, $\ell \in \mathbb{N}_0$ that is graded towards $\partial\Gamma$, *i.e.*, for all elements $T \in \mathcal{T}_\ell$ there holds

$$h_\ell(T) \simeq \operatorname{dist}(T, \Gamma)^\beta.$$

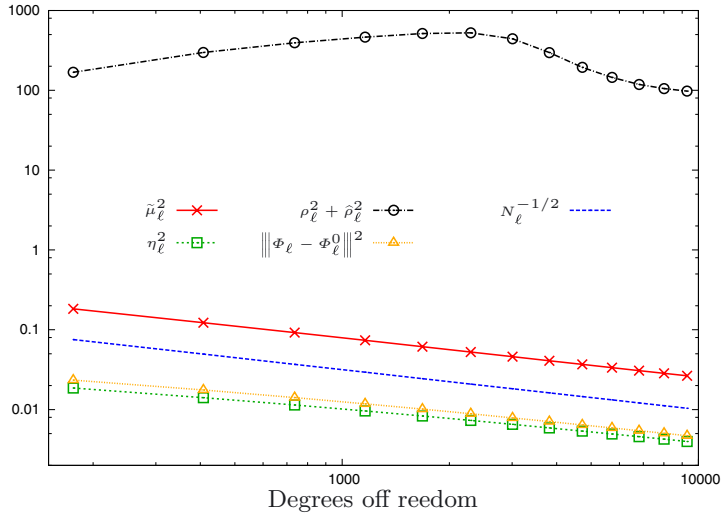

FIGURE 10. Convergence history for graded meshes with $\beta = 3$ and geometric singularities. The squared quantities exhibit the optimal rate $\mathcal{O}(N_\ell^{-1/2})$.

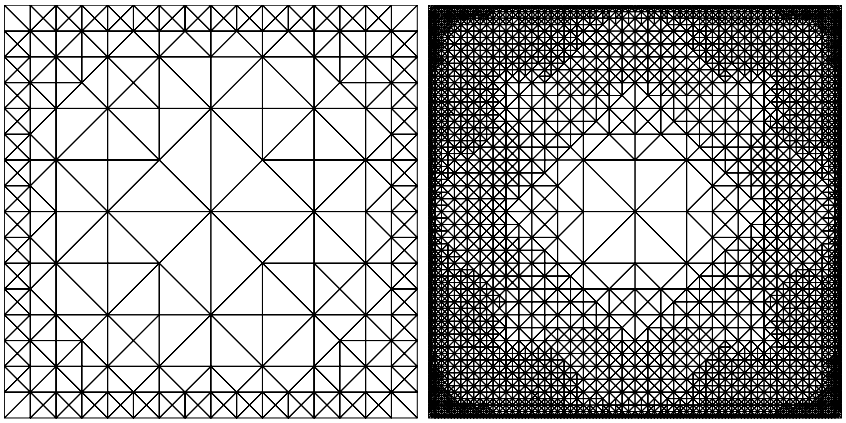

FIGURE 11. Meshes $\mathcal{T}_{11}$ and $\mathcal{T}_{21}$ of the adaptive Algorithm 1 with $\theta = 0.5$ for geometric singularities.

We select the parameters $\beta \in \{2, 3\}$. The numerical results show that both gradings maintain the conjectured optimal rate for the Crouzeix–Raviart BEM (see Figs. 9 and 10).

5.2. Experiment with singular solution

The right-hand side is given by

$$f(x, y) := x^{-6/10},$$

and because of $f \notin L_2(\Gamma)$ we conclude from the mapping properties of $\mathcal{W}$ that the exact solution fulfills $\phi \notin H^1(\Gamma)$. The missing regularity will lead to a suboptimal convergence rate for uniform refinement, which will be recovered by the adaptive algorithm. Let us briefly discuss what to expect in the uniform case: for the function $g(x) = x^\alpha$ there holds $g \in H^{\alpha+1/2-\varepsilon}(0, 1) \setminus H^{\alpha+1/2}(0, 1)$ for all $\varepsilon > 0$. We conclude that,

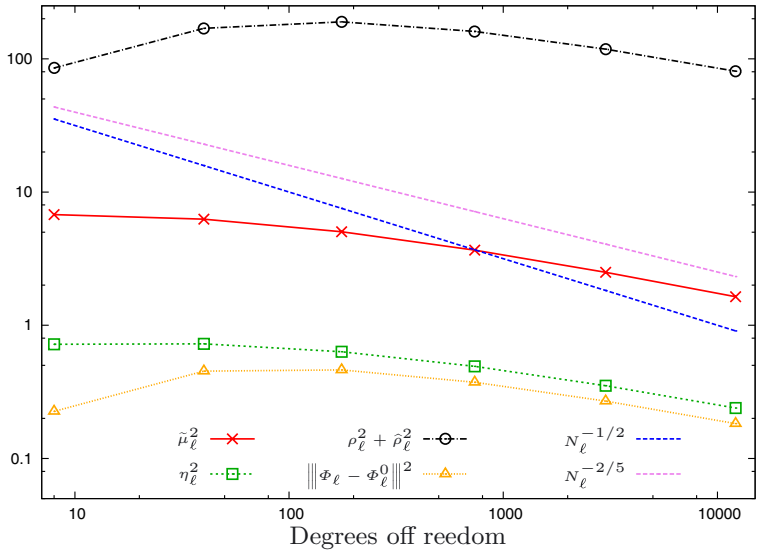

FIGURE 12. Convergence history for uniform mesh refinement and singular right-hand side. The squared quantities do not exhibit the optimal rate, which would be $\mathcal{O}(N_\ell^{-1/2})$.

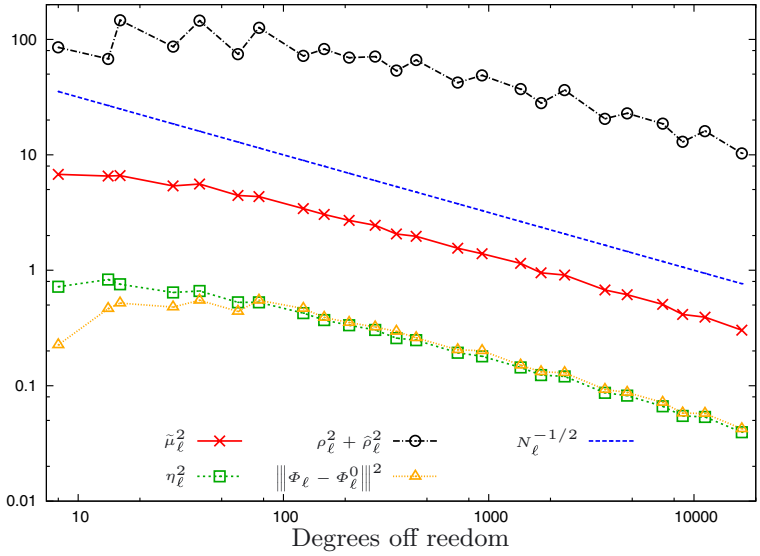

FIGURE 13. Convergence history for adaptive algorithm, $\theta = 0.5$, and singular right-hand side. The squared quantities exhibit the optimal rate $\mathcal{O}(N_\ell^{-1/2})$.

$f \in H^{-0.1-\varepsilon}(\Gamma) \setminus H^{-0.1}(\Gamma)$, and due to the mapping properties of $\mathcal{W}$ we conclude that $\phi \notin \widetilde{H}^{9/10}(\Gamma)$. Hence, we expect a convergence rate which is worse than $\mathcal{O}(h_\ell^{4/10}) = \mathcal{O}(N_\ell^{-1/5})$ for uniform refinement. We already stated the choice of the initial mesh $\mathcal{T}_0$. Uniform and adaptive meshes are computed exactly as described in Section 5.1. The convergence history for the uniform sequence of meshes is depicted in Figure 12. We see that the uniform scheme is suboptimal, and the convergence rate is indeed worse than $\mathcal{O}(N_\ell^{-1/5})$ (note that we plot squared quantities). However, the adaptive sequence of meshes, depicted in Figure 13, recovers the optimal convergence rate. In Figure 16, we plot the two adaptive meshes $\mathcal{T}_{11}$ and $\mathcal{T}_{23}$ which are generated by the adaptive

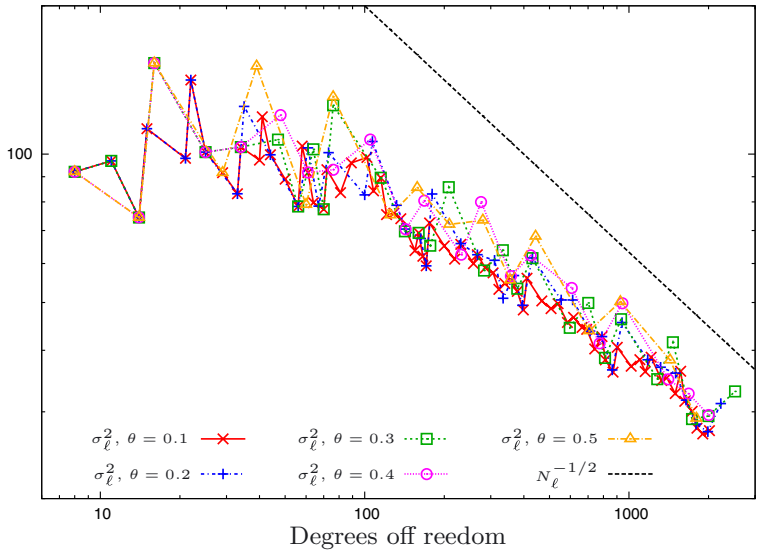

FIGURE 14. Error estimator σ_ℓ^2 for adaptive Algorithm 1 with different values of $\theta \in \{0.1, 0.2, 0.3, 0.4, 0.5\}$ and singular right-hand side. The squared quantities exhibit the optimal rate $\mathcal{O}(N_\ell^{-1/2})$.

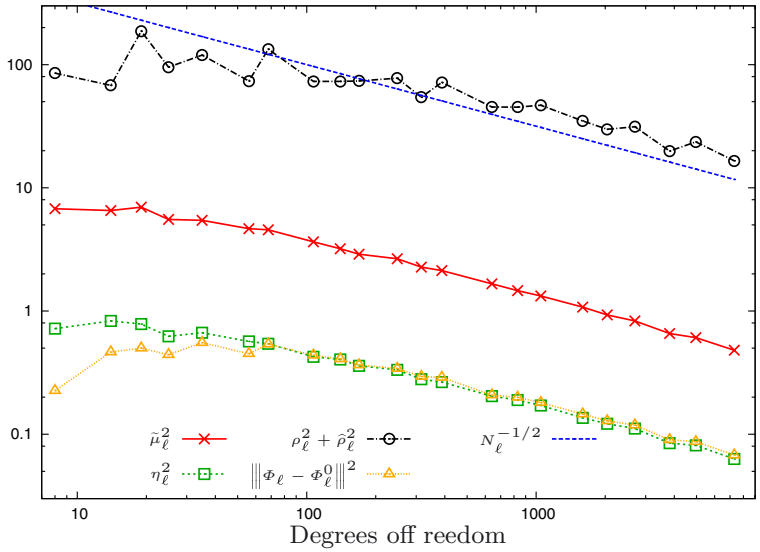

FIGURE 15. Convergence history for adaptive Algorithm 2 with separate marking and singular solution. The squared quantities exhibit the optimal rate $\mathcal{O}(N_\ell^{-1/2})$.

Algorithm 1. In Figure 14, we plot the error estimate σ_ℓ^2 *versus* the number of degrees of freedom for the choices $\theta \in \{0.1, 0.2, 0.3, 0.4, 0.5\}$. As in the first experiment, there is no substantial difference in this range of θ. The outcome of the adaptive Algorithm 2 with separate marking strategy and $\theta_1 = \theta_2 = \vartheta$ is shown in Figure 15. As in the first experiment, the jump terms $\rho_\ell^2 + \widehat{\rho}_\ell^2$ dominate the estimator $\widetilde{\mu}_\ell^2$ by one order of magnitude, such that only the marking (4.6b) takes place. The optimal order of convergence $\mathcal{O}(N_\ell^{-1/4})$ is recovered also in this case.

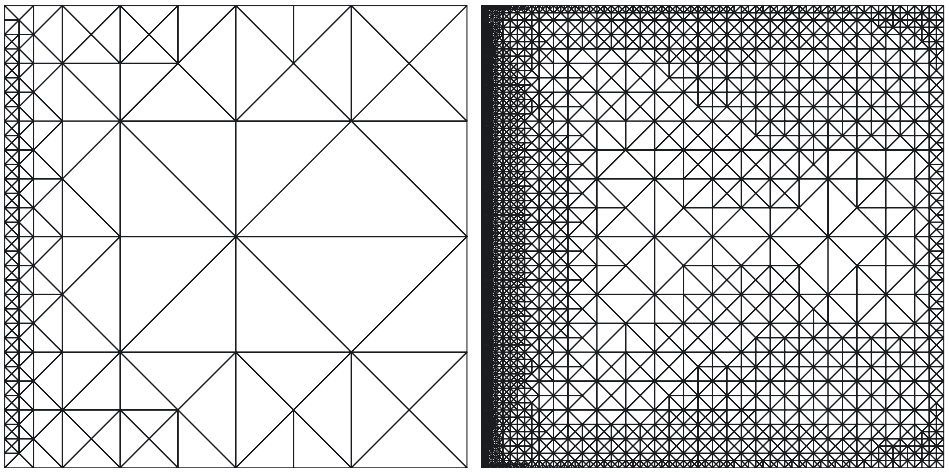

FIGURE 16. Meshes $\mathcal{T}_{11}$ and $\mathcal{T}_{23}$ of the adaptive Algorithm 1 with $\theta = 0.5$ for singular solution.

REFERENCES

[1] M. Ainsworth and J. Tinsley Oden, A posteriori error estimation in finite element analysis. *Pure Appl. Math.* Wiley-Interscience [John Wiley & Sons], New York (2000).

[2] M. Aurada, M. Feischl, T. Führer, M. Karkulik and D. Praetorius, Efficiency and Optimality of Some Weighted–Residual Error Estimator for Adaptive 2D Boundary Element Methods. *Comput. Methods Appl. Math.* **13** (2013) 305–332.

[3] M. Aurada, M. Feischl, T. Führer, M. Karkulik and D. Praetorius, Energy norm based error estimators for adaptive BEM for hypersingular integral equations. *Appl. Numer. Math.* (2014).

[4] R.E. Bank, Hierarchical bases and the finite element method. In vol. 5 of *Acta Numer.* Cambridge Univ. Press, Cambridge (1996) 1–43.

[5] A. Berger, R. Scott and G. Strang, Approximate boundary conditions in the finite element method. In vol. X, *Symposia Mathematica (Convegno di Analisi Numerica, INDAM, Rome, 1972).* Academic Press, London (1972) 295–313.

[6] A. Bespalov and N. Heuer, The *hp*-version of the boundary element method with quasi-uniform meshes in three dimensions. *ESAIM: M2AN* **42** (2008) 821–849.

[7] P. Binev, W. Dahmen and R. DeVore, Adaptive finite element methods with convergence rates. *Numer. Math.* **97** (2004) 219–268.

[8] A. Bonito and R.H. Nochetto, Quasi-optimal convergence rate of an adaptive discontinuous Galerkin method. *SIAM J. Numer. Anal.* **48** (2010) 734–771.

[9] A. Buffa, M. Costabel and D. Sheen, On traces for $\mathbf{H}(\mathbf{curl}, \Omega)$ in Lipschitz domains. *J. Math. Anal. Appl.* **276** (2002) 845–867.

[10] C. Carstensen and D. Praetorius, Averaging techniques for the a posteriori BEM error control for a hypersingular integral equation in two dimensions. *SIAM J. Sci. Comput. 29* (2007) 782–810.

[11] C. Carstensen, M. Maischak, D. Praetorius and E.P. Stephan, Residual-based a posteriori error estimate for hypersingular equation on surfaces. *Numer. Math.* **97** (2004) 397–425.

[12] Ph. Clément, Approximation by finite element functions using local regularization. *RAIRO Anal. Numér.* **9** (1975) 77–84.

[13] C. Domínguez and N. Heuer, A posteriori error analysis for a boundary element method with non-conforming domain decomposition. *Numer. Methods Partial Differ. Eq.* **30** (2014) 947–963.

[14] W. Dörfler, A convergent adaptive algorithm for Poisson's equation. *SIAM J. Numer. Anal.* **33** (1996) 1106–1124.

[15] W. Dörfler and R.H. Nochetto, Small data oscillation implies the saturation assumption. *Numer. Math.* **91** (2002) 1–12.

[16] Ch. Erath, S. Ferraz-Leite, S. Funken and D. Praetorius, Energy norm based a posteriori error estimation for boundary element methods in two dimensions. *Appl. Numer. Math.* **59** (2009) 2713–2734.

[17] V.J. Ervin and N. Heuer, An adaptive boundary element method for the exterior Stokes problem in three dimensions. *IMA J. Numer. Anal.* **26** (2006) 297–325.

[18] S. Ferraz-Leite and D. Praetorius, Simple a posteriori error estimators for the *h*-version of the boundary element method. *Computing* **83** (2008) 135–162.

[19] S. Ferraz-Leite, C. Ortner and D. Praetorius, Convergence of simple adaptive Galerkin schemes based on $h - h/2$ error estimators. *Numer. Math.* **116** (2010) 291–316.

[20] G.N. Gatica, M. Healey and N. Heuer, The boundary element method with Lagrangian multipliers. *Numer. Methods Partial Differ. Eq.* **25** (2009) 1303–1319.

[21] I.G. Graham, W. Hackbusch and S.A. Sauter, Finite elements on degenerate meshes: inverse-type inequalities and applications. *IMA J. Numer. Anal.* **25** (2005) 379–407.

[22] E. Hairer, S.P. Nørsett and G. Wanner, Solving ordinary differential equations. I, Nonstiff problems. In vol. 8 of *Springer Ser. Comput. Math.* Springer-Verlag, Berlin (1987).

[23] N. Heuer, On the equivalence of fractional-order Sobolev semi-norms. *J. Math. Anal. Appl.* **417** (2014) 505–518.

[24] N. Heuer and F.-J. Sayas, Crouzeix–Raviart boundary elements. *Numer. Math.* **112** (2009) 381–401.

[25] M. Karkulik, D. Pavlicek and D. Praetorius, On 2D Newest Vertex Bisection: Optimality of Mesh–Closure and H^1-Stability of L_2-Projection. *Constr. Approx.* **38** (2013) 213–234.

[26] W. McLean, Strongly elliptic systems and boundary integral equations. Cambridge University Press, Cambridge (2000).

[27] J.-C. Nédélec, Integral equations with nonintegrable kernels. *Int. Eq. Oper. Theory* **5** (1982) 562–572.

[28] E.P. Stephan, Boundary integral equations for screen problems in $\mathbb{R}^3$. *Int. Eq. Oper. Theory* **10** (1987) 257–263.

[29] L. Ridgway Scott and Shangyou Zhang, Finite element interpolation of nonsmooth functions satisfying boundary conditions. *Math. Comput.* **54** (1990) 483–493.

[30] R. Stevenson, Optimality of a standard adaptive finite element method. *Found. Comput. Math.* **7** (2007) 245–269.

[31] H. Triebel, Interpolation theory, function spaces, differential operators, 2nd edn. Edited by Johann Ambrosius Barth, Heidelberg (1995).

[32] R. Verfürth, A Review of A Posteriori Error Estimation and Adaptive Mesh-Refinement Techniques. B.G. Teubner, Stuttgart (1996).